© 2021 Elsevier Ltd. All rights reserved. This is the accepted manuscript version of an article which has been published in final form at https://doi.org/10.1016/j.asoc.2021.108072

Cooperative Relay Spectrum Sensing for Cognitive Radio Network: Mutated MWOA-SNN Approach

Geoffrey Eappen, Shankar T, and Rajagopal Nilavalan, *Member, IEEE*

Abstract

The spectrum overcrowding is one of the prime issues faced by wireless telecommunication based applications. The network blockage causing the disconnection or call drops is another important concern. These problems, are needed to be addressed for implementing the 5G and beyond technologies. Therefore, to tackle the issues of spectrum overcrowding and network blockage simultaneously a Cognitive Radio (CR) technology based relay network is proposed in this work. The accurate detection of the primary user's signal by the cognitive radio users is the most integral functioning of the cognitive radio networks. The existing spectrum sensing using Deep Neural Network (DNN) and Convolutional Neural Network (CNN) techniques have their limitations concerned with accurate prediction and classification of vacant spectrum due to their tendency of getting jammed to the local optima. In this paper, we firstly propose a novel mutated Modified Whale Optimization Algorithm (MWOA) trained Spiking Neural Network (SNN) based spectrum sensing technique for the efficient detection of spectrum holes. Here, the weights of the SNN are trained by means of MWOA for efficiently predicting the spectrum holes. The proposed scheme exploits underlying structural information of the sensed signals via continuous wavelet transforms. The proposed scheme does not require any priori information about the channel state and is shown to achieve state of the art performance in the detection of spectrum holes. The simulation results have inferred that the proposed CR based relay model with the MWOA trained SNN based spectrum sensing has significantly improved the performance of the User Equipment (UE) in the network blockage area in terms of higher opportunistic throughput and lower BER. The MWOA has proved to be an efficient training algorithm for SNN with the validation accuracy of 98%.

Index Terms

Spectrum Sensing, Cognitive Radio, Modified Whale Optimization Algorithm, Spiking Neural Network.

1 Introduction

The wireless IoT based applications in the present scenario play a pivotal role in enhancing the wellness of a population. But the network capacity of wireless telecommunication is reaching its maximum capacity [1]. In addition to that, Millimeter Wave (mmWave) frequency has high attenuation [61]. Such a scenario results in a network blockage condition. Therefore, the important concern to be addressed in the area of the 5G and beyond based communication technology is the network blockage resulting in the network disconnection due to the limited penetration ability of the radio waves. The inefficient usage of the radio spectrum by wireless communication technologies is another major concern in wireless communication services resulting in spectrum congestion. Therefore, in this paper, novel MWOA trained SNN based efficient spectrum sensing is employed for the CR relay network. The simulation results depicts the effectiveness of the proposed scheme with which it is possible to overcome the problems of wireless network blockage and

Geoffrey Eappen is with the Vellore Institute of Technology, Vellore, 632014 India (e-mail: geoffrey.eappen@vit.ac.in).
Shankar T is with the Vellore Institute of Technology, Vellore, 632014 India (e-mail: tshankar@vit.ac.in).
Rajagopal Nilavalan, is with Brunel University, London, UB83PH UK (e-mail: nila.nilavalan@brunel.ac.uk).

spectrum congestion.

Efforts are made to overcome above mentioned problems via employing techniques like carrier aggregation and Multiple Input Multiple Output (MIMO) antenna scheme [1]. In [2-4], authors employed space time block coding and Turbo coding schemes to improve the channel capacity via multipath wireless communication. These plans couldn't take care of the issue of network capacity, as channel limit cannot be expanded vastly by numerous antennae, which further results in extra costs.

A relay based wireless system in which UE act as a relay to another UE symbolizing Device to Device (D2D) communication is studied in [5]. The prime advantage of the D2D communication is the improvement in the network connection of the UE which is experiencing network blockage. Furthermore, it does not incur additional costs to the wireless operators for setting up the relay BS establishment [21] [57]. One of the drawbacks associated with UE and UE based relay networks is that the UE relays are not stationary and there are possibilities of UE relays themselves getting stuck to some network blockage condition. Moreover, the increasing demands in the D2D based application can further escalate the network congestion and spectrum scarcity problems which can cause reduced data rate and enhanced latency [22] [23].

To tackle such issues, a CR based relay system is proposed to establish a link from UE to its Base Station (BS) and vice versa. In this work, MWOA is employed in training the SNN for efficiently classifying the channel based on the presence and the absence of the licensed users and detecting the spectrum holes even at low SNR values. The reason for choosing SNN over DNN or CNN is because the SNN exactly mimic the human brain [32]. For 5G spectrum sensing it is important to process spatial and temporal data and SNN has proven ability to process spatial and temporal data efficiently [38] [65]. Moreover, in this paper, the proposed scheme employs real time spectrum sensing using USRPs. For real-time USRP based spectrum sensing it is important to consider different factors that contribute in its performance. From [67] [68], it is infered that the influence of the modelling errors, calibration, device's disturbance and choice of filtering techniques have impact on the efficiency of USRP based real time spectrum sensing. In this work, the real time issues associated with the device is considered while modelling the proposed MWOA-SNN based spectrum sensing via USRPs. To avoid the inaccuracies associated with USRPs proper terminations of transmit and receive ports are performed. Calibration errors of the USRPS are rectified by handling the mother board with anti static methods and avoiding voltage spikes [72]. Also, to mitigate the non linear distortion in the receiver, the Finite Impulse Response Filter (FIR) with adaptive filter coefficients is implemented [73]. Another important factor considered in this work is the employmnet of the soft computing scheme. While incorporating a metaheuristic trained Artificial Intelligence (AI) scheme for a real time applications it is important to consider that the complexity associated with the AI scheme does not cause latency issue. Specifically when the AI scheme is employed for 5G techniques with multi users, latency is an important factor to be considered. Therefore, the complexity and the associated latency are crucial limitations associated with AI schemes applied for real applications for 5G technology. To solve this problem, this work carries out MWOA-SNN training in the offline mode and the trained MWOA-SNN is then applied for the real time spectrum hole detection. Hence, the complexity and the latency associated with the training of the SNN is limited only to the training phase and it does not impact the complexity during the working phase on the spectrum sensing efficiency [66]. Throughout the paper, the base station corresponding to the UE is denoted as BS and the base station corresponding to the Licensed User (LU) is denoted as LU_{BS}. The CR based relay network can potentially prove as effective in overcoming the fading problem in D2D communication by providing high channel capacity with low cost [22] [23]. In the previous work [57], relay based cognitive radio network was developed employing a weighted cooperative spectrum sensing (CSS) scheme with MWOA optimization. In this paper effort is made to develop a novel MWOA trained SNN for spectrum hole detection for a relay based cognitive radio network.

The organization of this paper is as follows: Related works that have been surveyed are mentioned in Section 2. The proposed work's design, how the study is carried and data were analyzed are discussed in Section 3 System Modelling. The existing SNN, drawbacks associated with it and the objective function for training

the SNN are discussed in Section 4. Section 5 discusses about mathematical modelling corresponding to the opportunistic throughput and CWT. In Section 6 proposed MWOA is discussed. A detailed description of the proposed MWOA training of SNN is carried out in Section 7. Simulation results and its discussions are detailed in Sections 8 and 9, followed by the conclusion in Section 10.

2 Literature Survey

A CR network can adapt and allocate dynamically different spectrum resources to the cognitive radio users/ secondary users via efficient spectrum sensing and sharing [6]. The CR network forms an important part of the digital transformation in this pandemic situation and does an impact on all fields [71]. In addition to that it can also change its working variables like power, modulation scheme, carrier frequency to adapt to the learning environment [69]. In [23], implemented the CR for relay networks via conventional energy detection technique for spectrum sensing. The conventional energy detection techniques for spectrum sensing is the least complex but suffers at low SNR [6]. The soft computing techniques like ANN, Fuzzy Logic, DNN and CNN are very popular because of their abilities to efficiently recognize or classify the data set [29], [30], [62], [63], [64]. But the existing neural network scheme with back propagation is based on gradient decent method which has the drawback of getting stuck to the local optima [31]. The fuzzy logic proves to be an efficient soft computing scheme in finding the stability of controller systems [70]. But the accuracy of the fuzzy logic is compromised as the system operates on inaccurate data and inputs [70]. The metaheuristic trained ANN has constrained computational performance because of the limitations associated with its metaheuristic approaches [61]. The developed ANN is said to mimic the functionality of the brain but still, it is in its initial state of exactly mimicking the brain functionality [32]. The computational ability of the brain is based on its distributed network of neurons linked to each other via synaptic connections. The SNN is based on the spikes generated between neurons connected via synapses. It has the potential to mimic the computational and intelligence ability much closer to a brain's intelligence [32]. Therefore SNN is more effective in classification problems as compared to conventional ANN and CNN [32].

The conventional SNN is based on fixed connection weights and networks [33]. As per Hebbian theory, a brain operates with optimal networking between co-active cells [34]. Therefore, an optimal weight connection is desirable and it is an important research problem. The issue associated with the deployment of the dynamic synapse is optimizing the synaptic parameter. Genetic algorithm and evolutionary algorithms have been employed for solving this issue. The idea for the swarm based training for the SNN is inspired by the work in [38]. The SNN training using swarm intelligence was successfully implemented in [38]. But the employed optimization algorithm is the conventional PSO, which has the drawback of getting converged to the local optima [12]. Therefore, in this work, a new and improved MWOA is employed for better training of the SNN.

The proposed scheme is compared with the existing Particle Swarm Optimization (PSO), Particle Swarm Optimization Gravitational Search Algorithm (PSOGSA), Advanced Squirrel Algorithm (ASA) and Gravitational Search Algorithm (GSA) based CR network. The PSO, GSA, and its modified version (PSOGSA) are extensively employed for spectrum sensing [24] [25] [26] [27]. The prime drawback associated with these algorithms is that they are capable of finding a very good solution but they converge before obtaining a global optimum solution [28] [61]. For spectrum sensing, it is very important that the algorithm does not converge to the near global solution but should obtain a global optimum solution to avoid interference with the PU and to carry out the remaining process of a CR network i.e opportunistic data transmission, spectrum sharing, spectrum mobility more effectively [58].

3 System Modeling

Figure 1 infers that when a UE is in the network blockage region or technically termed as the "dead zones" (Areas where mobile phone signal strength is measured in dBm is very low and the mobile phones are

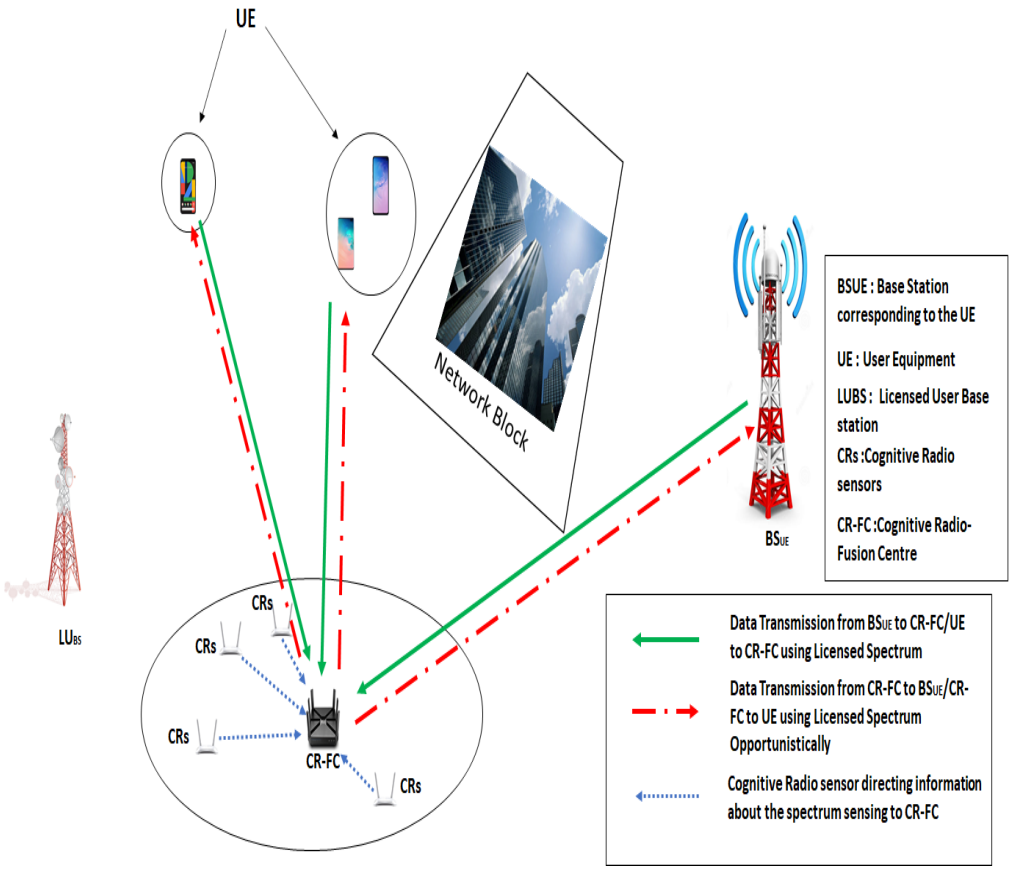

Fig. 1: Flow diagram of the proposed model

unable to establish link with nearby cellphone site, base station or repeater). Which causes the disruption in the link between UE and BS. A disruption in the link can affect the network performance. But the presence of deployed Cognitive Radio-Fusion Center (CR-FC) as the relay between UE and BS, UE and UE can remarkably enhance the network performance. The CR-FC is assisted with the Cognitive Radio Sensors (CRs) in a cooperative manner as shown in Figure 16. The detailed working on how CRs assists CR-FC via performing cooperative spectrum sensing is explained in section V(A). In the proposed scheme it is considered that a BS has the prior information about the nearby CR-FC in a specific geological area. The CR-FC can set up an appropriate connection with the BS in an opportunistic manner via vacant spectrum holes. On account of network blockage during downlink, the BS conveys to CR-FC via licensed spectrum. The CR-FC with the help of CRs performs spectrum detection to identify the active and the inactive state of the other nearby Licensed Users (LUs) in a specific topographical area. Once the vacant spectrum is detected, then the data is transmitted to the UE by craftily accessing the spectrum holes. In this way, via CR-FC the link is established between BS and UE. Only CR-Fc is accessing the licensed spectrum opportunistically, i.e. via detected spectrum holes as shown by dashed red line in Figure 1. One of the LUs considered in this work is the TV broadcast system and the role of CR-FC is to efficiently detect the vacant spectrum/TV white spaces. It is also considered that the UEs have the information of the nearby CR-FC and possesses the ability of transmitting data to the CR-FC via licensed spectrum. The CR-FC then again performs spectrum sensing and detect spectrum holes for opportunistically accessing the licensed spectrum and transmits data to the BS. Thus establishing UE-BS link. Similarly, a CR-FC based relay can act as a link for transmission and reception of data between different user equipment pertaining to the same region where network is blocked. The CR-FC can also communicate with other CR-FCs deployed in the specified

region to have better network coverage.
The efficient spectrum sensing for the proposed relay based CR network is designed using MWOA trained SNN. For training MWOA SNN, real time data is firstly obtained via USRP based spectrum sensing. These data carries the information about the presence and the absence of the PU. On these spectrum sensed signals, CWET is applied to obtain the wavelet coefficients. These wavelet coefficients are converted to scalograms and then into image of size 224x224x3. The convolutional MWOA SNN is trained to classify the images based on the presence and absence of PUs. The efficiency of conventional SNN is improved by incorporating the mutated MWOA during the training process. Its detailed description is presented in the section 4.3. In the working phase, i.e for the real time efficient spectrum sensing, the pre-trained convolutional MWOA-SNN is employed. The MWOA-SNN predicts the labels by feeding on the scalogram images. The data is analyzed via continuous wavelet analysis to classify the PU signals via trained MWOA SNN. Figures 24-27 show the accuracy and error deviation of each applied algorithm during the training phase of SNN. The Table 1 showcases the prime symbols and their notations involved in this work.

TABLE 1: Symbol Notations

Symbols	Description
CR-FC	Cognitive Radio-Fusion Center
UE	User Equipment
M	No of orthogonal subcarriers
W	Bandwidth of each subcarrier
CRs	Cognitive radio sensors
$h_{j,k,t}^{B,CRFC}$	The channel gain between BS and CR-FC over k^{th} subcarrier at time slot t
$h_{j,k,t}^{CRFC,UE}$	The channel gain between CR-FC and jt̂h UE over k^{th} subcarrier at time slot t
$Pwp_{j,k,t}^{B,CRFC}$	The BS to CR-FC transmission power
CR_p	The transmission power of CR-FC
CR_p^r	The CR-FC power received at UE
g_a	The CR-FC antenna gain
Pr^{LoS}	The LoS probability between CR-FC and UE
Pr^{NLoS}	The NLoS probability between CR-FC and UE
$Lo_{dB,LoS}^{UE}$	The path loss in dB for the LoS
$Lo_{dB,NLoS}^{UE}$	The path loss in dB for the NLoS

3.1 Major Contributions

The prime research objectives achieved in this paper is discussed as below:

1. **Proposed and developed CR based relay network with efficient spectrum sensing via SNN trained with MWOA** to simultaneously tackle problems of spectrum overcrowding and network blockage in a wireless communication network.
2. **Developed a novel training for the SNN via employing MWOA optimization for the weights of the SNN:** This work involves improving the efficacy of the conventional Spiking Neural Network (SNN) by employing Modified Whale Optimization Algorithm (MWOA). As the conventional SNN lacks the proper tuning of the weights of the synapses [38]. So, the MWOA based weight optimization for SNN is implemented in this paper. From the best of authors' knowledge, till now no works have been carried out for training an SNN using MWOA and employing it for CR spectrum sensing. This work is novel and also tested for real time scenario via USRPs. Therefore, the proposed scheme can be effectively employed in real time applications.
3. **Implemented modification to the conventional whale optimization algorithm via mutation and also by maintaining an expert balance between its exploration and exploitation ability** This

novel work involves the modification via mutation scheme to improve the conventional WOA, as it has the tendency of getting stuck to the local optima [12] [61].

4. **Implemented MWOA trained SNN for efficient real time spectrum senisng via USRPs:** With the proposed mutated MWOA, there is less possibility of it getting stuck to the local optima solution. Therefore, it is possible to achieve rapid and accurate classification of wireless channel occupancy via efficient optimization of weights for SNN using MWOA. Moreover, the proposed scheme is implemented for the popular wireless communication paradigm i.e spectrum sensing in cognitive radio network in a real time scenario. And this is the first of its kind work which has implemented MWOA trained SNN for spectrum sensing in cognitive radio network via USRPs. The proposed scheme has efficiently worked for the applied scenario as compared to its counter part as indicated in the simulation results.

4 THE SPIKING NEURAL NETWORK

The SNN is the class of neural network that employs a more efficient way for denoting biological neural networks for activating the neurons as compared to ANN (Feedforward Neural Network and Recurrent Neural Network) [35]. The architecture of the SNN closely relates to the biological neural network model [32] [35]. The SNN is an efficient way for the classification of the images. But it lacks optimal weight connection for efficient classification [33]. In this paper, MWOA is employed in finding the optimal weight links between the neurons of the SNN to enhance its efficiency. The proposed SNN is employed for classifying the images generated from the spectrogram, and the continuous wavelet transform is employed for this purpose. The Continuous Wavelet Transform (CWT) is employed on PU signals and is converted in the time-frequency domain known as scalograms. The precomputing scheme of the CWT filter bank is used for obtaining the CWT of the PU signals. The detailed working of the wavelet transform for classifying the PU signals is explained in section V Mathematical Modeling.

Hyper-parameters of SNN:

$y, z, \ and \ x -$ Synaptic resource fraction in the active, inactive and recovered state.
$t^{sp} -$ Time for presynaptic spike reaching synapse
$U^{SE} -$ Synaptic Efficiency
$\tau^{m} -$ Time coonstant for membrane
$\tau^{rec} -$ Time span for synaptic recovery
$I_{i}^{syn} -$ The synaptic efficiency in receiving current
$A^{SE} -$ Absolute synaptic efficiency
$R^{in} -$ Membrane potential
$w_{m}^{ij} -$ The weight associated with each synaptic terminal
$\mathrm{Y}_{m}^{i} -$ Unweighted contribution of each spike

4.1 Related works in SNN

SNNs are employed in different successful applications [39] [40]. The use of SNN becomes more influential when the training data is continuous and varying in time [38]. The reason is that in SNN the information is encoded in time i.e. Spike Time Dependent Plasticity (STDP), dynamic synapse model [41]. The STDP employs synaptic weight varying with respect to time correlation between spikes of the pre and the postsynaptic neuron. The STDP is based on Hebbian unsupervised learning approach, in which its dynamic parameters are kept fixed and weight is altered [38]. One of the prime drawback associated with STDP is that it is flexible with only one tunable parameter. To overcome this issue, genetic algorithm and evolutionary algorithm based strategies are used in [41] [42] [43]. In [41], authors employed SNN

for classifying static data. The initial progress in supervised training technique was based on gradient descent for SNN was developed in [44], popularly known as SpkieProp. The SpikeProp was successful in overcoming the issues associated with the conventional SNN. But the drawback associated with the SpikeProp is that its neuron are allowed to fire once. Therefore, SpikeProp could not become feasible for training patterns comprising multiple spikes [41]. In [45], the probabilistic gradient descent approach was considered which comprised biological window for learning. As this approach also uses single spikes so it is not feasible for training patterns comprising multiple spikes.
An optimization algorithm to be employed for training SNN should be capable of updating weights based on the error deviation in the correlation between firings of the post and the presynaptic neurons [47]. Therefore, in this work, SNN weighted links are optimized to have minimized error deviation between its classified and target values.

4.2 The Basic functioning of SNN based on its neuron and synapse

The brain functioning is based on the magnitude change of the postsynaptic neuron with respect to the firing pattern of the presynaptic neuron.

Dynamic synaptic models utilizing the phenomenon of the brain are proposed in [48] [49] [50] resulted in the development of SNN. The use dependency for generating the postsynaptic potentials (PSP) depends on the available resource's amount [32] [51]. The model utilizing the PSP generation based on the available resources was briefly described in [50]. A portion of the available resources is utilized whenever a presynaptic spike reaches synapse. The model in [50] considered finite resources for the neurons. The presynaptic spike reaching synapse at time t^{sp} will be utilizing U^{SE} amount of synaptic efficiency [50] and it quickly inactivate within the time span of τ^m and recovers back within τ^{rec}. The kinetic equation involved in this model can be written as [50]:

$$\frac{dx}{dt} = \frac{z}{\tau^{rec}} - U^{SE}\delta(t - t^{SP}) \tag{1}$$

$$\frac{dy}{dt} = -\frac{y}{\tau^m} + U^{SE}\delta(t - t^{SP}) \tag{2}$$

$$\frac{dz}{dt} = \frac{y}{\tau^m} - \frac{z}{\tau^{rec}} \tag{3}$$

Here, y, z , and x represents synaptic resource fraction in the active, inactive and recovered state respectively.
The synaptic efficiency in receiving current from synapse i to the postsynaptic neuron can be written as [32]:

$$I_i^{syn} = A^{SE} y_i(t) \tag{4}$$

here, A^{SE}: Absolute synaptic efficiency (Resembles when all of the resources are activated).
The popular firing model considered in this paper is Leaky Integrate and Fire (LIF). The LIF is modeled as below [36]:

$$\tau^m \frac{\partial v}{\partial t} = -v + R^{in} I^{syn} \tag{5}$$

here, R^{in}: Membrane Potential
τ^m: Membrane time constant. The Figure 2 and 3 show the LIF generated for the step and the sinusoidal input current. The python based Brian2 platform is employed for generating the LIF model in figures 1 and 2.

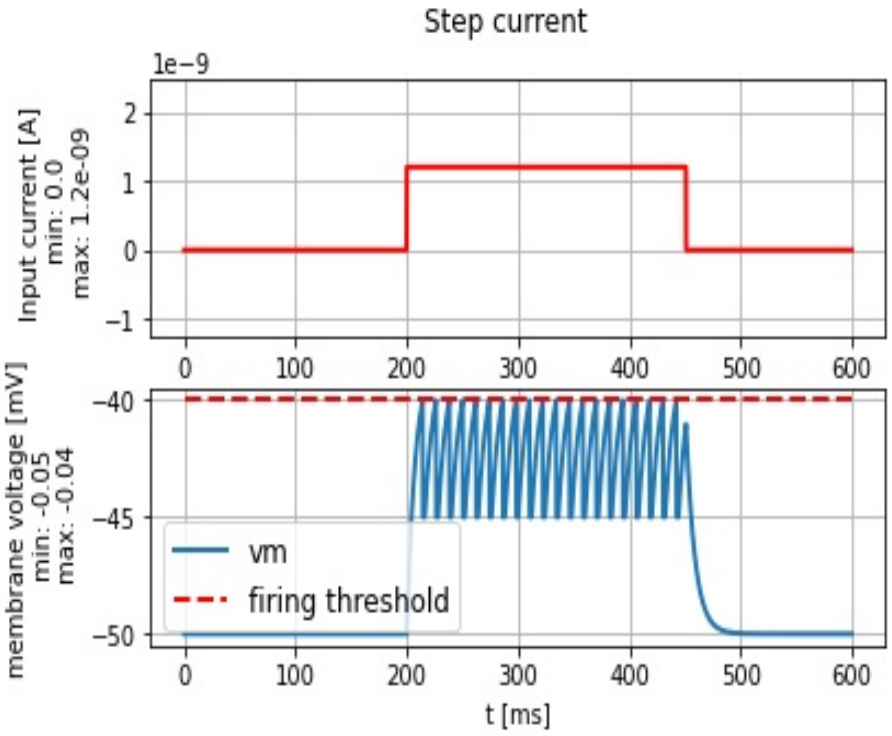

Fig. 2: LIF for the step input current

4.3 Objective Function for Training the SNN

In this paper, MWOA is employed for training the SNN by optimizing its weight values. The SNN weights get updated based on the error deviation between target spike sequence and the input spike sequence. MWOA is employed to minimize this error deviation and improve the correlation between target spike sequence and the input spike sequence. The minimized error deviation between the spike sequence of the target and the input spike train is highly desirable.

The Figure 4 shows the schematic diagram of the two neurons i and j having K synaptic terminals between them. The input neuron i receives spike train at time instant t^i. The neuron j fires only when the membrane voltage level crosses the threshold. The effective weighted contribution of spikes between neuron i and j can be modeled as [54]:

$$x^j(t) = \sum_{m=1}^{K} \mathrm{Y}_m^i w_m^{ij} \tag{6}$$

where, w_m^{ij} is the weight associated with each synaptic terminal between i and j, Y_m^i is the unweighted contribution of each spike. The $\mathrm{Y}_{\mathrm{m}}^{\mathrm{i}}$ can be written as [54]:

$$\mathrm{Y}_m^i = \Psi(t - t_i - d_m) \tag{7}$$

where, d_m: Delay between i and j nodes at the m^{th} synaptic terminal. Further, $\Psi(t)$ is calculated as $\frac{t}{\tau^m} e^{1-\frac{t}{\tau^m}}$. Here, τ^m is the time constant associated with membrane potential decay.

The SNN considered in this paper for predicting the presence and the absence of the PU comprises of an input layer for spectrogram images of size 224x224x3. The CWT is employed to the real time spectrum sensing results obtained via USRP N210 and B210 to obtain the spectrogram images as shown in Figure 6. The architecture for the proposed convolutional SNN is shown in Figure 5.

The proposed scheme's working model is as shown in Figure 6. For simplicity the images were rescaled to 28x28 with anti-aliasing effect. Therefore the input network has 784 neurons. The input network neurons

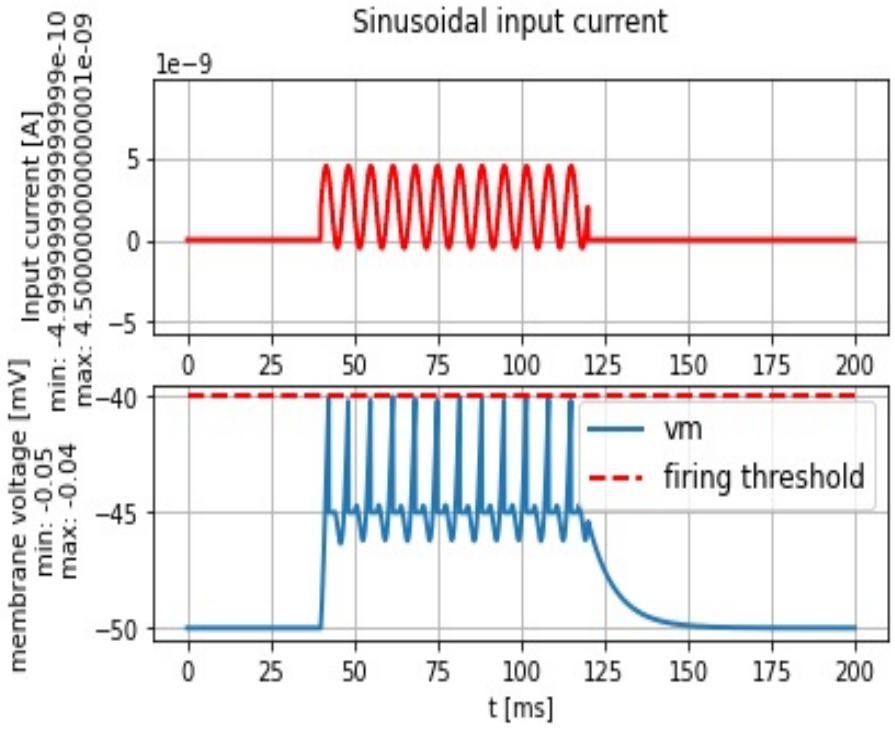

Fig. 3: LIF for the sinusoidal input current

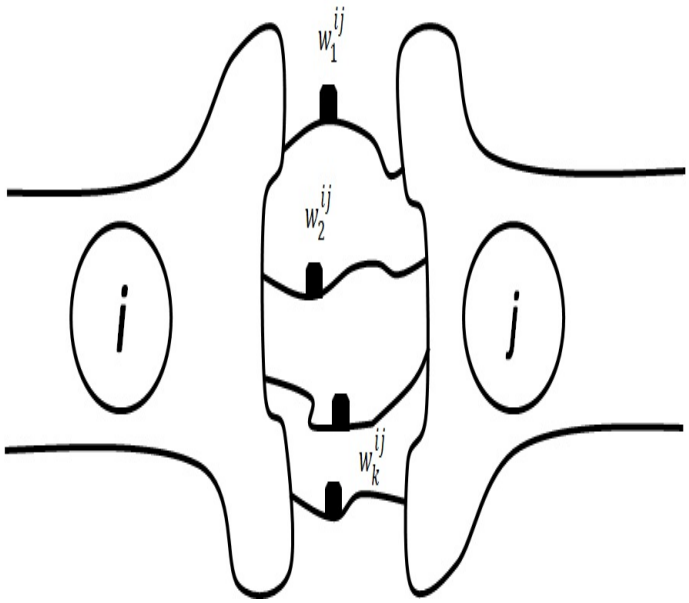

Fig. 4: LIF for the sinusoidal input current

are connected to hidden layer neurons via 12 convolutional kernels, each sized 5x5. The weighted synaptic connection between hidden convolutional layer and the output layer is trained/optimized via proposed MWOA. The input layer also comprises the spike train generated based on the scalogram images of the PU signal.

The steps involved in the SNN training is discussed below:

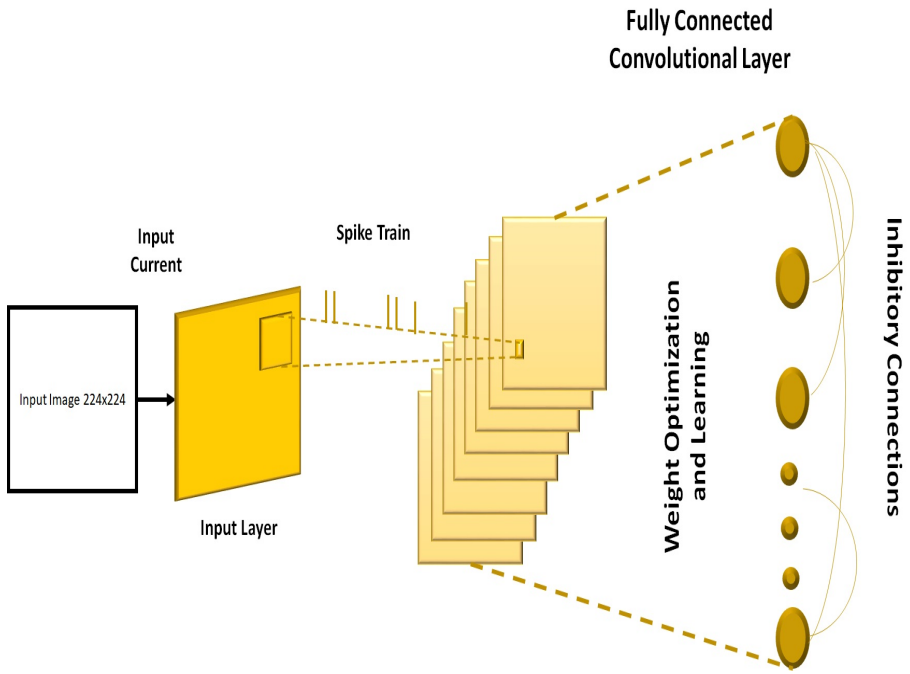

Fig. 5: Convolutional SNN Architecture

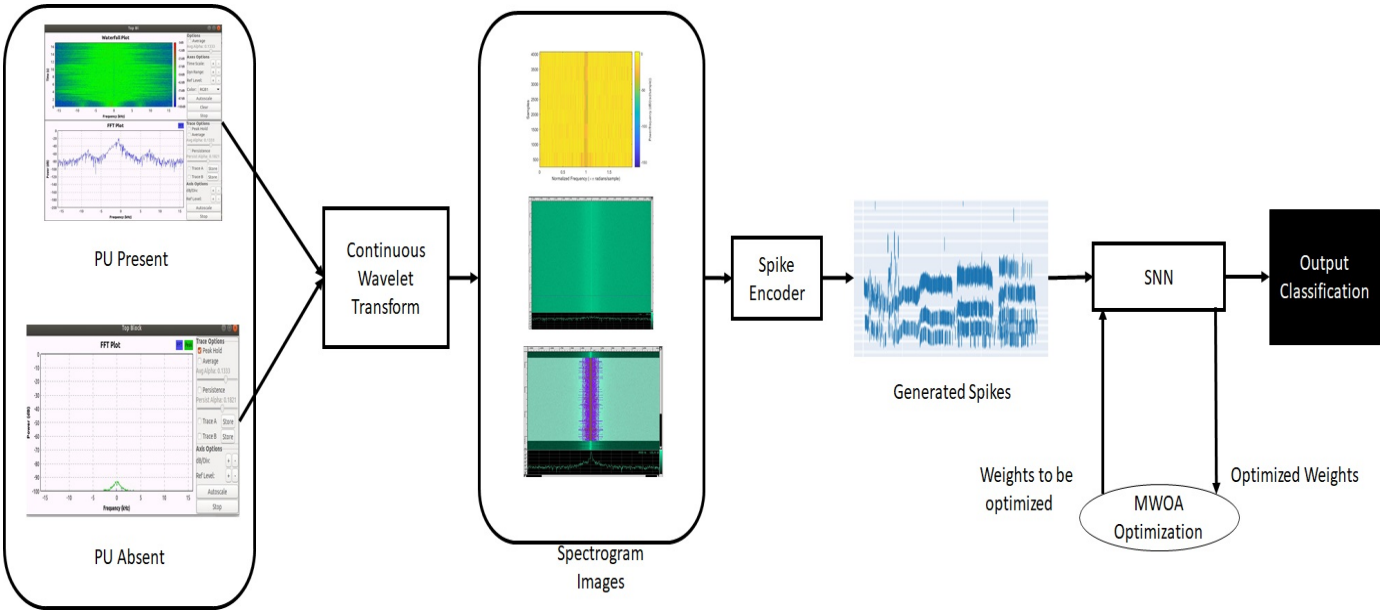

Fig. 6: Proposed scheme's working model

1. Scalegram based dataset is prepared for the scenario concerning the presence and the absence of the PU.

2. Generate the spike train sequence based on the firing rate proportional to each pixel value.

3. Randomly initialize weight values for the 1st epoch.

4. Initialize values for the parameters (Decay time constant= 10 ms, threshold membrane potential = 7 mV, reset voltage = 0.05 mV).

5. Considering the input layer as i, hidden layer as j and the number of output layers as o. The neurons count in each layer is indicated as $p^{'}$, $q^{'}$, and $o^{'}$ respectively.

6. Push the spike train into the network. Calculate the effective weighted contribution of the spikes between input and the hidden layer neurons at hidden layer neurons:

$$x^j(t) = \sum_i \sum_{m=1}^{K} \mathrm{Y}_m^i w_m^{ij} \tag{8}$$

7. Similarly calculate the effective weighted spike contribution between hidden layer and output layer at the output layer neurons:

$$x^o(t) = \sum_j \sum_{m=1}^{K} \mathrm{Y}_m^j w_m^{jo} \tag{9}$$

8. Objective Function: Calculating the error in the time difference between the actual and the desired spike timing is done as: $\varepsilon = \frac{1}{2}\sum_{o=1}^{o^{'}}(t_a^o - t_d^o)$. This error deviation also termed as loss in this paper is the objective function for the optimization problem solved via proposed MWOA.
9. Based on the similarity error/loss move the MWOA search agents in the mathematical search space of the ε for the change in weights.
10. Perform spiral and encircling mechanisms as discussed in section VI to obtain the optimal value of the weight change.
11. Feed the optimized weights to the SNN and calculate the value of ε.
12. Repeat the steps 9 to 11 until the minimized value of ε is reached.

To have better insight about the working of the proposed SNN, the internal working figures of the SNN is plotted and shown in figures 7-14. The figures 7 to 9 shows the rate of population of Xe, Ae, and Ai. The rate of population basically indicates the instantaneous firing rate averaged across the neurons with respect to the time step of the source clock. Here Xe is the input neurons. The Ae and Ai are the hiddenlayer neuron groups with 400 neurons each. The brian 2 simulator [59] is employed for generating the plots figures 7-14. The Figure 10 and 12 show the spikes recorded from the neuron groups Ae and Ai respectively.

The weight connections in figures 12, 13, and 14 show the weighted connections between Ae-Ai, Ai-Ae, adn Xe-Ae respectively.

5 Mathematical Modeling for the Opportunistic Throughput and Continuous Wavelet Transform

The calculation of the opportunistic throughput considers transmission of data from BS to CR-FC, and from CR-FC to UE.

Considering j^{th} UE facing the problem of network blockage in a 3D plane as shown in the Figure 15. The orthogonal subcarrier is represented as $k = 1, 2, 3...M$, each of bandwidth = W. The subcarriers are employed for resource allocation in CR-FC and BS. The proposed model comprises CRs as $l = 1, 2, 3, ...CR_s$. The data from each CRs is fed to the fusion center CR-FC for the final decison on the vacant spectrum. The CR-FC and CRs combinedly form the relay for assisting data transmission between BS to UE and UE to BS. For the data transmission to the j^{th} UE, which is in network blockage, the channel gain represented as $h_{j,k,t}^{B,CRFC}$ is the channel gain for the data transmission from the BS to CR-FC via subcarrier k and time slot t. The channel for the data transmission from CR-FC to UE j is denoted as $h_{j,k,t}^{CRFC,UE}$. The BS to CR-FC transmission power can be written as $Pwp_{j,k,t}^{B,CRFC}$. The transmission power of the CR-FC is fixed to CR_p.

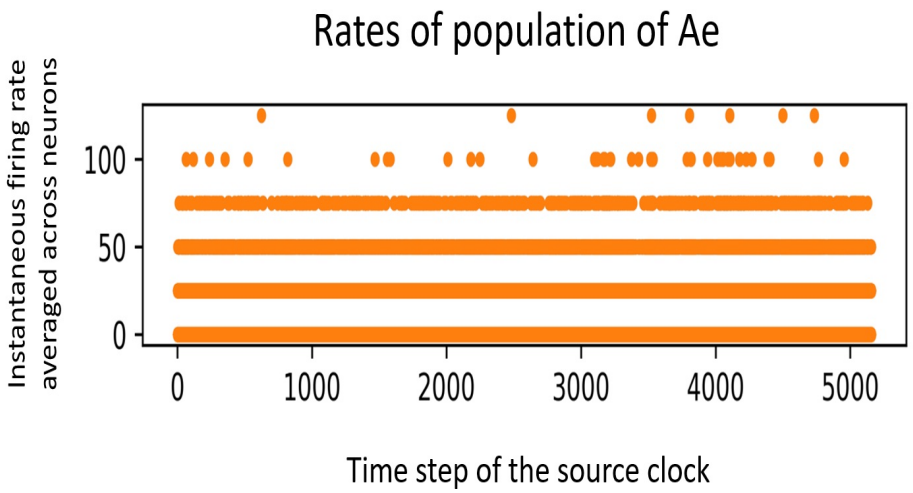

Fig. 7: Rates of Population of Ae

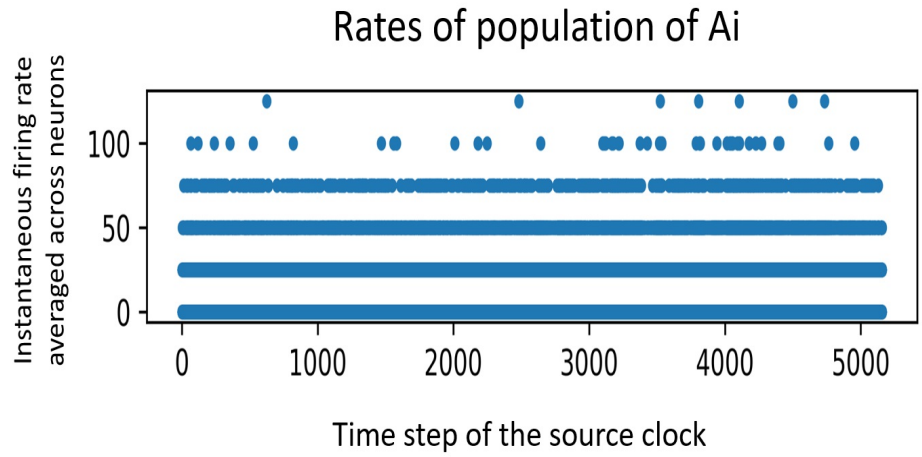

Fig. 8: Rates of Population of Ai

The BS power received at CR-FC can be estimated as Eq.10 [13]:

$$Pwp_{j,k,t}^{B,CRFC,r} = Pwp_{j,k,t}^{B,CRFC} \times \left\{ \frac{4\pi f_c d_o}{c} \right\}^{-2} \times d_{BS}^{-n'} \tag{10}$$

here, f_c is the licensed carrier frequency associated with the BS, d_o is a reference distance, d_{BS} is the distance between BS and the CR-FC calculated as $\sqrt{(x_{BS} - x^{CRFC})^2 + (y_{BS} - y^{CRFC})^2 + (h_{BS} - h)^2}$, (x_{BS}, y_{BS}, h_{BS}) is the coordinates associated with the BS location, n' is the path loss exponent. The transmission power CR_p of CR-FC at some height h as shown in Figure 15 is different from the CR-FC power received at UE CR_p^r. The coordinates of UE $j \in \ell$ is (x_j, y_j) and the coordinates of CR-FC is (x^{CRFC}, y^{CRFC}, h). For the communication link between CR-FC and UEs, the CR-FC with directional antenna with half beamwidth φ_{hbw}. The CR-FC antenna gain can be denoted as [13]:

$$g_a = \begin{cases} g_a^{3dB} & \frac{-\varphi_{hbw}}{2} \leq \psi \leq \frac{\varphi_{hbw}}{2} \\ g_{ao}(\psi) & otherwise \end{cases} \tag{11}$$

here ψ is the sector angle, $g_a^{3dB} \approx \frac{29000}{\varphi_{hbw}^2}$, φ_{hbw} in degree is the gain of the main lobe [14], $g_{ao}(\psi)$ is the gain outside the main lobe. Because of the uncertainity associated with the UE location, height and the

Fig. 9: Rates of Population of Xe

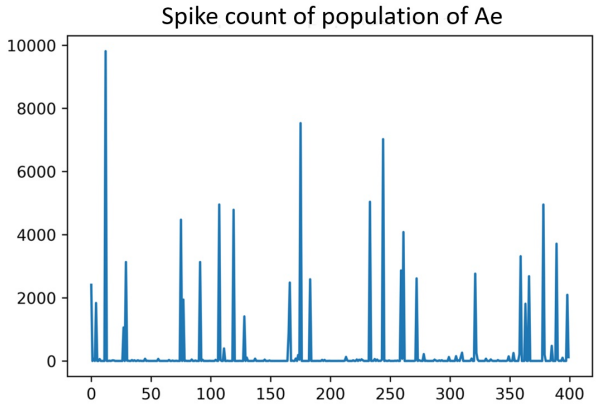

Fig. 10: Spike Count of Population of Ae

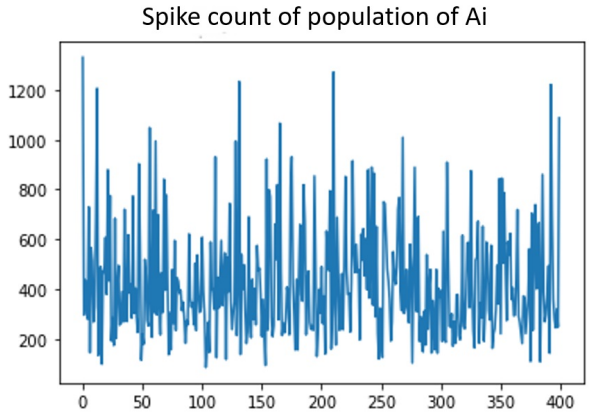

Fig. 11: Spike Count of Population of Ai

obstacles, it is important to consider the randomness in the link between CR-FC and UE and also vice versa. Therefore, the link between CR-FC and UE can be of Line of Sight (LoS) and Non Line of Sight (NLoS) with certain probabilities [16].

As per the 3GPP 3D model of the Urban Macro scenario for the UE of height 1.5m [15], the LoS probability between CR-FC and UE can be modelled as [16] [18] [20]:

$$Pr^{LoS} = \frac{1}{1 + \alpha \times exp(-\beta \left|\theta_j - \alpha\right|)} \tag{12}$$

here α, β are the constants corresponding to carrier frequency and the environment type like rural, urban, and urban dense, $\theta_j = \frac{180}{\pi} \times sin^{-1}(\frac{h}{d_j})$, d_j is the distance between CR-FC and UE, calculated as $\sqrt{(x_j - x^{CRFC})^2 + (y_j - y^{CRFC})^2 + h^2}$.

The probability of NLoS is as in Eq.(13):

$$Pr^{NLoS} = 1 - Pr^{LoS} \tag{13}$$

The maximum coverage of a base station antenna with beamwidth φ_b is given as $r_a = h \times tan(\frac{\varphi_{hbw}}{2})$ [17]. For the transmission power of CR_p, the received power of CR-FC at j^{th} UE for the LoS and NLoS link is

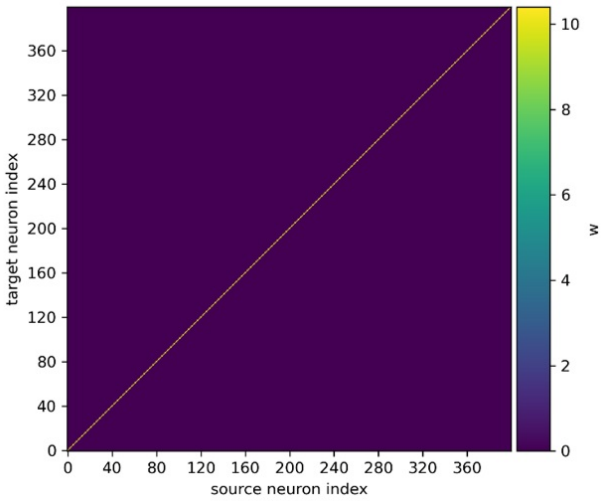

Fig. 12: Weight Connection AeAi

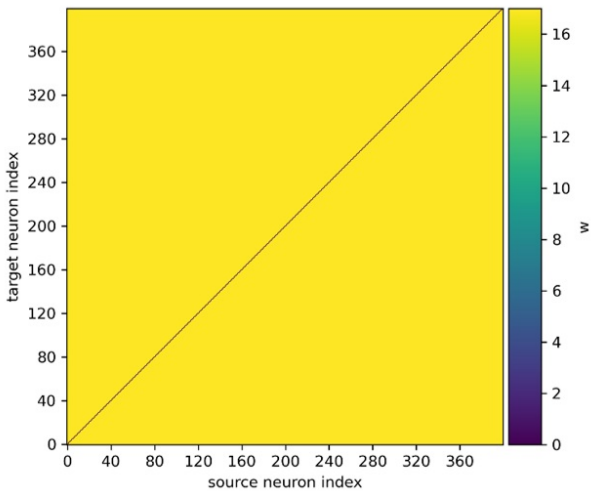

Fig. 13: Weight Connection AiAe

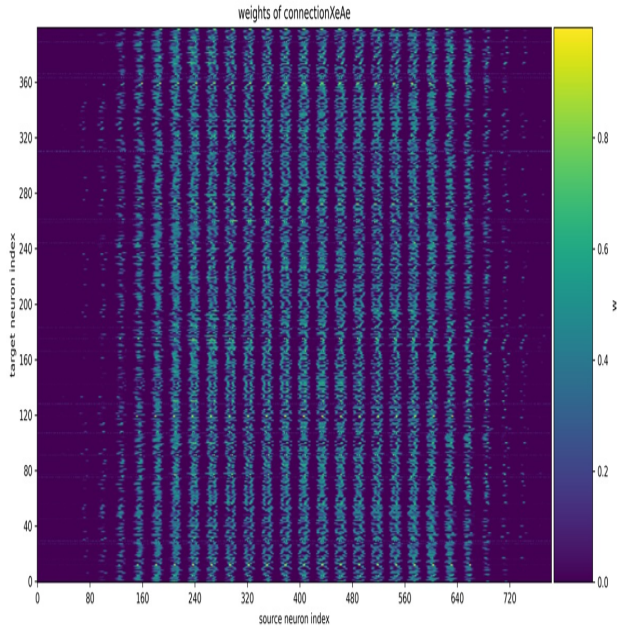

Fig. 14: Weight Connection XeAe

given as in Eq.(14):

$$CR_p^r = \begin{cases} CR_p + g_a^{3dB} - Lo_{dB,LoS}^{UE} - E_{LoS}, & \text{LoS Link} \\ CR_p + g_a^{3dB} - Lo_{dB,NLoS}^{UE} - E_{NLoS}, & \text{NLoS Link} \end{cases} \tag{14}$$

For a fixed location of CR-FC and varying locations of the UEs the path loss associated with this situation is to be considered averaged path loss. Therefore, The path loss in dB for the LoS and NLoS is given as $Lo_{dB,LoS}^{UE}$ and $Lo_{dB,NLoS}^{UE}$ respectively. The path loss between CR-FC and UE is calculated as in Eq.(15):

$$Lo_{dB}^{UE} = \begin{cases} Pr^{LoS}\Upsilon_1 \left\{ \frac{4\pi f_s^c d_j}{c} \right\}^{n'}, & \text{LoS Link} \\ Pr^{NLoS}\Upsilon_2 \left\{ \frac{4\pi f_s^c d_j}{c} \right\}^{n'}, & \text{NLoS Link} \end{cases} \tag{15}$$

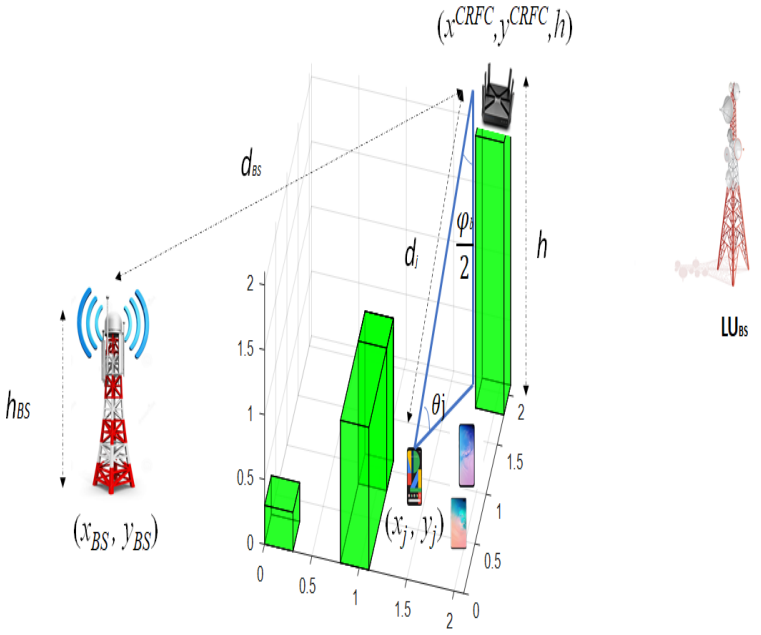

Fig. 15: Detailed representation of the proposed model

where, f_s^c is the spectrum sensed carrier frequency of the CR-FC, n' is the path loss exponent, d_i is the distance between CR-FC and UE and c is the speed of light, Υ_1, Υ_2 are the coefficients of the excessive path loss during LoS and NLoS conditions respectively.
The shadow fading in dB for the LoS and NLoS link is denoted as E_{LoS} and E_{NLoS} respectively. The E_{LoS} and E_{NLoS} has the normal distribution as $E_{LoS} \sim \mathbb{N}(\mu_{LoS}, \sigma^2_{LoS})$, $E_{NLoS} \sim \mathbb{N}(\mu_{NLoS}, \sigma^2_{NLoS})$ respectively. The μ_{LoS}, μ_{NLoS} are the mean. The $\sigma_{LoS}, \sigma_{NLoS}$ (variance) depends on environmental condition and the elevation angle as denoted in Eqs.(16) and (17) [18]:

$$\sigma_{LoS} = J_1 e^{(-J_2\theta_j)}, \tag{16}$$

$$\sigma_{NLoS} = G_1 e^{(-G_2\theta_j)} \tag{17}$$

where, J_1, J_2, G_1, G_2 are the constants depending on environmental constraints. The received j^{th} UE power at CR-FC is calculated as in Eq.(18). The link between CR-FC and BS can be modeled as in Eq.(19), the received CR-FC power at BS is estimated as in Eq.(19).

$$Pwp_{j,k}^{UE,CRFC,r} = \begin{cases} Pwp_{j,k}^{UE,CRFC} - Lo_{dB,LoS}^{UE} - E_{LoS}, & \text{LoS Link} \\ Pwp_{j,k}^{UE,CRFC} - Lo_{dB,NLoS}^{UE} - E_{NLoS}, & \text{NLoS Link} \end{cases} \tag{18}$$

$$CR_{p,BS}^{r} = CR_p \times \left\{ \frac{4\pi f_c d_o}{c} \right\}^2 \times d_{BS}^{-n'} \tag{19}$$

The opportunistic throughput $T_{j,k}^{h,B-UE}$ evaluated for CR-FC assisted data transmission between the BS and the UE denoted as j is as shown in Eq.(20)[5][7]:

$$T_{j,k}^{h,B-UE} = \frac{1}{2} log_2 \left\{ 1 + \frac{Pwp_{j,k,t}^{B,CRFC,r} \times CR_p^r \times h_{j,k,t}^{B,CRFC} \times h_{j,k,t}^{CRFC,UE}}{(N_0 W) \times (Pwp_{j,k,t}^{B,CRFC,r} \times h_{j,k,t}^{B,CRFC} + CR_p^r \times h_{j,k,t}^{CRFC,UE})} \right\} \tag{20}$$

The power spectral density of the noise is denoted as N_0. A unit buffer size is assumed for the time index therefore it is omitted. Hence, Eq.(20) can be re-written as Eq.(21):

$$T_{j,k}^{h,B-UE} = \frac{1}{2} log_2 \left\{ 1 + \frac{Pwp_{j,k}^{B,CRFC,r} \times CR_p^r \times h_{j,k}^{B,CRFC} \times h_{j,k}^{CRFC,UE}}{(N_0 W) \times (Pwp_{j,k}^{B,CRFC,r} \times h_{j,k}^{B,CRFC} + CR_p^r \times h_{j,k}^{CRFC,UE})} \right\} \tag{21}$$

The opportunistic throughput for the CR-FC assisted transmission of data between UE and BS is formulated as in Eq.(22):

$$T_{j,k}^{h,UE-B} = \frac{1}{2} log_2 \left\{ 1 + \frac{Pwp_{j,k}^{UE,CRFC,r} \times CR_{p,BS}^r \times h_{j,k}^{UE,CRFC} \times h_k^{CRFC,BS}}{(N_0 W) \times (Pwp_{j,k}^{UE,CRFC,r} \times h_{j,k}^{UE,CRFC} + CR_{p,BS}^r \times h_k^{CRFC,BS})} \right\} \tag{22}$$

where the transmission power denoted as $Pwp_{j,k}^{UE,CRFC}$ is the power employed for the transmission of data by the j^{th} UE. The $h_{j,k}^{UE,CRFC}$ denotes channel gain between UE j and the CR-FC. The $h_k^{CRFC,BS}$ is the channel gain between CR-FC and BS.

5.1 CSS Model

This work considers the CSS scheme as show in the Figure 16. The SNN of each CRs is first trained using the different scalograms for the presence and the absence of the PUs. The training is done in the offline mode, the trained SNN CRs are then employed in the online mode for the real time classification of the presence and the absence of the PUs. The prediction is made in terms of 1s and 0s for the presence and the absence of the PUs respectively. The value is fed to CR-FC to make the final decision on the channel state.

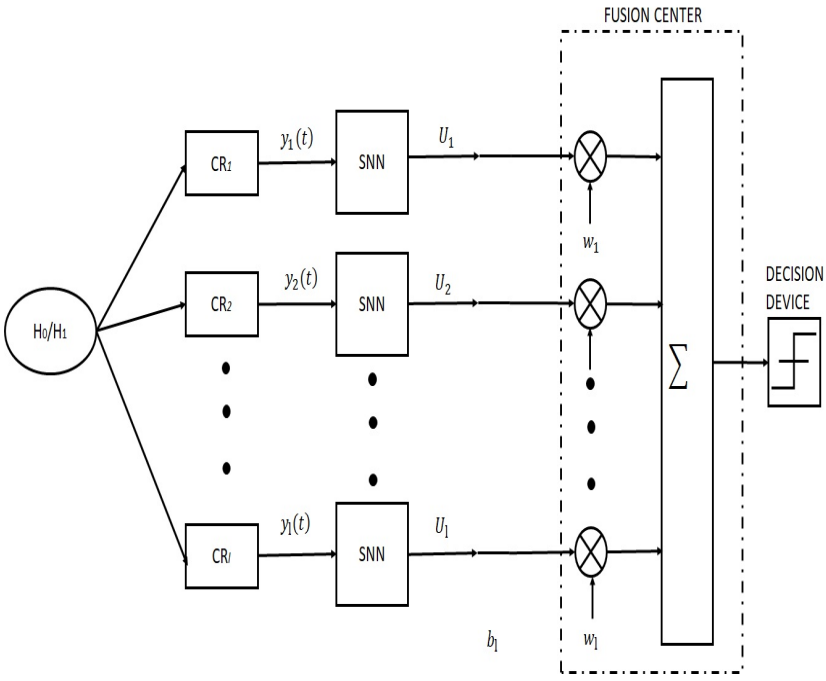

Fig. 16: Cooperative spectrum sensing model

The mathematical modelling and the calculation for the opportunistic throughput with respect to the probability of detection and false alarm probability is as explained in our previous work in [27] [46]. The hypothesis for the employed Spectrum Sensing is as denoted by the Eq.(23) [46]:

$$\begin{aligned} &\mathrm{H}_0 : y_l(t) = n_l(t) && \{(\text{PU Absent})\} \\ &\mathrm{H}_1 : y_l(t) = h_l s(t) + n_l(t) && \{(\text{PU Present})\} \end{aligned} \tag{23}$$

here, $y_l(t)$: Sensed sample at the l^{th} CRs for the time instant t, here $t = 0, 1, 2..N-1$.
h_l: Channel gain at CRs l.
$s(t)$: LU/PU signal.
$n_l(t)$: Noise received at CRs l having zero mean and variance σ_l^2.
The test statistics for spectrum sensing at each CRs is calculated as in Eq.(24):

$$U_l = \sum_{t=0}^{N-1} |y_l(t)|^2 \tag{24}$$

At fusion center: $\{z_l\}_{l=1}^{CRs}$, where $z_l = U_l + b_l$, b_l is the control channel noise between l^{th} CRs and CR-FC. The b_l is AWGN with 0 mean and variance v_l^2.
The weighted value at fusion center is estimated as in Eq.(25):

$$\sum_{l=1}^{CRs} w_l z_l = \mathbf{w}^T \mathbf{z} \tag{25}$$

where, $\mathbf{w} = [w_1, w_2, w_3, ...w_{CRs}]^T$
$\mathbf{z} = [z_1, z_2, z_3, ...z_{CRs}]^T$
$[.]^T$:Matrix Transpose.
The accurate detection probability is estimated as in Eq.(26) [8][9]:

$$P^d = Q\left(\frac{Q^{-1}(P^f)\sqrt{\mathbf{w}^T\mathbf{C}\mathbf{w}} - e_s[\mathbf{h}]^T\mathbf{w}}{\sqrt{\mathbf{w}^T\mathbf{D}\mathbf{w}}}\right) \tag{26}$$

where, $Q(x) = \frac{1}{\sqrt{2\pi}}\int_x^\infty e^{-a^2/2}da$, $e_s = \sum_{t=0}^{N-1}|s(t)|^2$,
$\mathbf{h} = [|h_1|^2, |h_2|^2, ... |h_{CRs}|^2]^T$
$\mathbf{C} = 2N \times diag^2(\sigma) + diag(v)$,
$\mathbf{D} = 2N \times diag^2(\sigma) + diag(v)$
$+4e_s \times diag(\mathbf{h}) + diag(v)$.
here diag(.) represents diagonal matrix.
$\sigma = [\sigma_1^2, \sigma_2^2, ...\sigma_{CRs}^2]^T$, $v = [v_1^2, v_2^2, ...v_{CRs}^2]^T$.
Similarly the false alarm probability is estimated as Eq.(27):

$$P^f = Q\left(\frac{Q^{-1}(P^d)\sqrt{\mathbf{w}^T\mathbf{D}\mathbf{w}}}{\sqrt{\mathbf{w}^T\mathbf{C}\mathbf{w}} - e_s[\mathbf{h}]^T\mathbf{w}}\right) \tag{27}$$

With the help of Eq.(21), the achievable throughput is calculated and employed for simulation shown in figures 29 and 30. Its estimation for the transmission of data from BS to UE via CR-FC is as in Eq.(28):

$$T_{j,k}^{ach,B-UE} = P^{H_0}(\frac{t^f - t^s}{t^f})(1 - P^f)T_{j,k}^{h,B-UE} \tag{28}$$

here, the frame duration = t^f t^s = sensing time and P^{H_0} = probability of PU's inactivity.
Similarly, for UE to BS it is estimated as shown in Eq.(29):

$$T_{j,k}^{ach,UE-B} = P^{H_0}(\frac{t^f - t^s}{t^f})(1 - P^f)T_{j,k}^{h,UE-B} \tag{29}$$

5.2 CWT of the PU Signals to generate its scalogram images

In this paper, the received or spectrum sensed signals are first represented in the time frequency format. Such time frequency representation of signal is called as scalograms. Figures 17-19 show the scalogram for the PU. The scalograms are obtained via employing CWT. The absolute value of CWT coefficient is utilized as scalogram. The CWT filterbank precomputation is performed to generate scalogram. These scalogram images are then fed to the SNN for the training. The CWT is mathematically represented as [55]:

$$CWT_{\psi}^{Y}(A,B) = \frac{1}{\sqrt{(|A|)}} \int_{-\infty}^{\infty} Y(t)\psi(\frac{t-B}{A})dt \tag{30}$$

The $\psi(t)$ is dependent on A:Scaling parameter(controls the frequency of the wavelet function) and B: Shifting Parameter and it is represented as $\psi_{A,B}(t) = \psi(\frac{t-B}{A})$. An ideal $\psi(t)$ should have mean 0 and its ends must be decaying quickly [55].

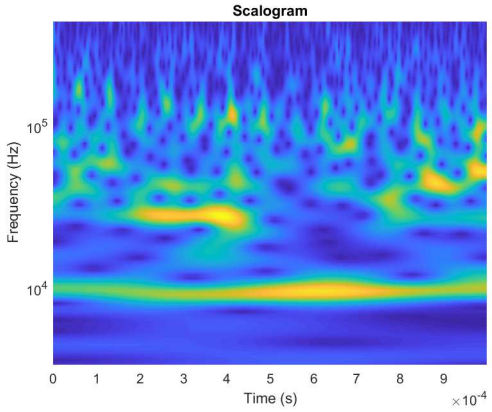

Fig. 17: Scalogram for PU spectrum

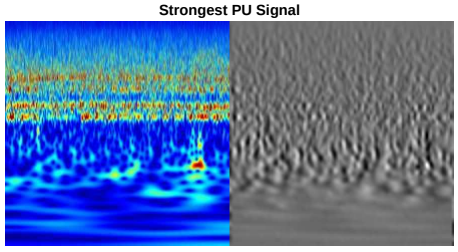

Fig. 18: The scalogram and the grey scale image obtained for the Strongest PU signal

6 MWOA:The Proposed Optimization Scheme

6.1 The Conventional WOA

Mimicking the hunting behavior of the whales, the WOA was developed in 2016 [10]. The three important mechanisms involved in WOA are random search phase, spiral position update technique, and encircling mechanism for finding an optimum solution. The three techniques are explained in brief as below:
Encircling Mechanism: Based on the objective function as discussed in the point 8 under the section IV(C) and the constraints ($\sum_{l=1}^{CRs} w_l = 1$, and $0 \leq w_l \leq 1$), the search agents are first randomly initialized. After

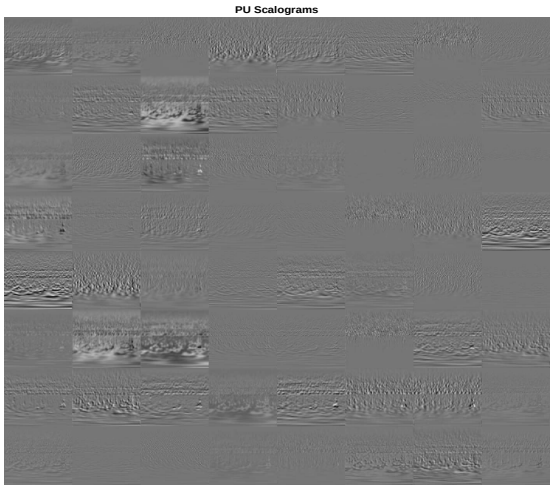

Fig. 19: PU Scalograms

obtaining the fitness value for each search agents then in the encircling mechanism, the whales/search agents update their position as in Eq.(31) and Eq.(32) [10] [58]:

$$\vec{\mathrm{D}} = \left| \vec{\mathrm{C}} \cdot \vec{X}_n^* - \vec{X}_n \right| \tag{31}$$

$$\vec{X}_{n+1} = \vec{X}_n^* - \vec{\mathrm{A}} \cdot \vec{\mathrm{D}} \tag{32}$$

here, $\vec{\mathrm{D}}$ is the distance vector of the new solution from a prey position, $\vec{\mathrm{C}}$ is the coefficient vector and it is equal to $2 \cdot \vec{r}$, for the current iteration n (n=0, 1, 2...n_{max}) prey's position vector or the position vector of the best solution obtained so far is represented as X_n^*. The position vector of the search agent for the next iteration is represented as $\vec{X}_{n+1}$. The $\vec{\mathrm{A}}$ is termed as discrimination weight coefficient and is calculated as in Eq.(33):

$$\vec{\mathrm{A}} = |2\vec{a} \cdot \vec{r} - \vec{a}| \tag{33}$$

here $\vec{a}$ is varied from 2 to 0 as a linearly declining vector, $\vec{r}$ is a random vector having values between 0 and 1.

For the $p \leq 0.5$ and $|A| \leq 1$, the encircling mechanism is initiated. Here p is a random number generated between 0 and 1 for each iteration.

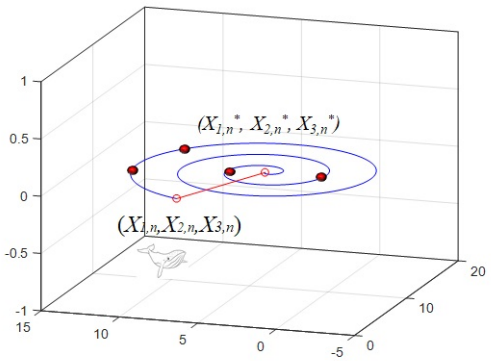

Fig. 20: 3D representation of the Encircling position update of the search agent (Whale) towards the best solution

The Figure 20 shows the pictorial representation of the encircling mechanism of the WOA.

Spiral Position Update Technique: The condition for the spiral update scheme is $p > 0.5$. In this technique the search agents move in the direction of the prey/best solution as a spiral shape. The Figure 21 shows the 3D representation of the spiral position updates of the whales towards the best solution $(X^*_{1,n}, X^*_{2,n}, X^*_{3,n})$ of a 3 dimensional problem. The equation governing this technique is as in Eq.(34) and Eq.(35):

$$\vec{X}_{n+1} = \vec{D} \cdot e^{bl} \cdot cos(2\pi l) + \vec{X}^*_n, \;\; l \in [-1, 1] \tag{34}$$

$$\vec{\mathrm{D}} = \left| \vec{X}^*_n - \vec{X}_n \right| \tag{35}$$

Here, b is a constant for defining the logarithmic spiral shape and l is a number varying randomly between [-1,1].

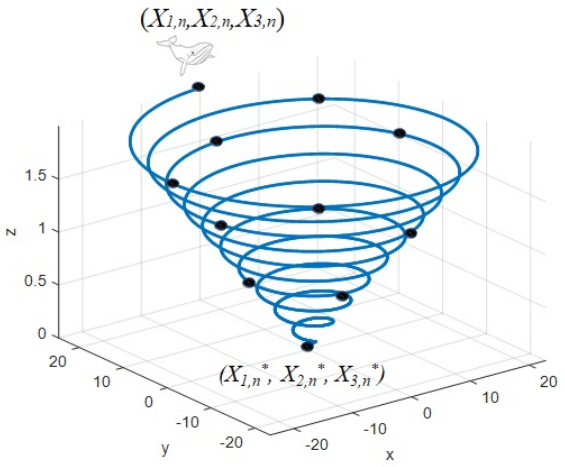

Fig. 21: 3D representation of the spiral position update of the search agent (Whale) towards the best solution

Random Search Phase: This mechanism is important for WOA to carry out proper exploration and have good global search.

The random global search is initiated when the $p \leq 0.5$ and $|A| > 1$. In this phase, emphasis is made on random solution selection instead of exploiting the local best solution The mathematical equations governing this search is as shown in Eq.(36) and Eq.(37):

$$\vec{\mathrm{D}} = \left| \vec{\mathrm{C}} \cdot \vec{X}^{rand}_n - \vec{X}_n \right| \tag{36}$$

$$\vec{X}_{n+1} = \vec{X}^{rand}_n - \mathrm{A} \cdot \vec{\mathrm{D}} \tag{37}$$

6.2 Modifications to implement Expert balance between Exploration and Exploitation of WOA

A balance between global and local search is very important for the optimization algorithm [12]. The local search/exploitation is performed well by the WOA, but the global search/exploration is carried out by randomly assigning search agent position irrespective of its position from the best solution. The drawback of such a random search is that it might be in the already searched region i.e a local optima. Such drawbacks associated with the WOA call for the need for its modification [60]. To avoid getting stuck to local best solution and to enhance the global search ability, in MWOA, a threshold is introduced to select search agent as a random pick. For enhanced global search it is important that the search agent must explore the unexplored regions. Therefore, in MWOA the search agents which are not nearby to the current best

solution are selected for the random search. In this way, the solutions which are in unexplored region is preferred for initializing the global search.
Modification can be mathematically modeled as in equations (38 to 41):

$$d_1 = \left| \vec{X}_n^* - \vec{X}_n^{rand} \right| \tag{38}$$

$$d_2 = \left| \vec{X}_n^* - \vec{X}_n^{best_2} \right| \tag{39}$$

where, $\vec{X}_n^{best_2}$ is the 2nd best solution among all the search agents.
If $d_1 > d_2$, and $p \leq 0.5$ and $|A| > 1$ then update search agents as:

$$\vec{\mathrm{D}} = \left| \vec{\mathrm{C}} \cdot \vec{X}_n^{rand} - \vec{X}_n \right| \tag{40}$$

$$\vec{X}_{n+1} = \vec{X}_n^{rand} - \vec{\mathrm{A}} \cdot \vec{\mathrm{D}} \tag{41}$$

And if $d_1 < d_2$, then select the next random search agent, continue this process until the condition $d_1 > d_2$ is satisfied. The proposed modification via Eqs.(38-41) can be termed as *Modified Random Search Phase*.

For an optimization algorithm it is important that its search agents reach almost all possible solution in the search space without slowing down the entire search process [19]. So, in this paper Mutation and Replacement strategy is applied. In each iteration, the search agents undergoes mutation and the corresponding solution then replaces the worst solution in the solution set to make sure that the search agents overcome local optima and progresses towards global best solution. In this way, the entire search agents would be led towards the global optimum solution in an efficient manner.

After *Encircling Mechanism / Spiral Update Mechanism* and *Modified Random Search Phase*, the search agents undergoes Polynomial Mutation Scheme, in which offspring is generated based on Eq.(42):

$$\vec{X}_n^{mut} = \vec{X}_n + (\vec{X}_n^U - \vec{X}_n^L)\delta_n \tag{42}$$

here, $\vec{X}_n^U$ and $\vec{X}_n^L$ are the upper and lower bounds of X_n. The δ_n is computed via employing polynomial probability distribution model [45]:

$$P(r_n) = 0.5(\eta^m + 1)(1 - |r_n|^{\eta^m}) \tag{43}$$

$$\delta_n = \begin{cases} 2r_n^{\frac{1}{(\eta^m+1)}} - 1, & u < 0.5 \\ 1 - 2(1 - r_{f,n})^{\frac{1}{(\eta^m+1)}}, & \text{otherwise} \end{cases} \tag{44}$$

where, η^m is generally ≈ 20 and u is random number ranging in [0,1]. Based on fitness of the solutions the search agents are categorized and the worst solution is replaced by the mutated solution $\vec{X}_n^{mut}$. The proposed MWOA has efficient exploration scheme with which random search agent are selected such a way as shown in equations (38-41) that it overcomes local optima. With polynomial mutation scheme as described in equations (42-44) the proposed MWOA has double edge sword of efficient tradeoff between exploration and exploitation therefore it converge towards the global optimum solution as shown in figures 20 and 21.

7 PROPOSED MWOA TRAINED SNN

In this paper, MWOA is employed for training the SNN. The SNN training using swarm intelligence was successfully implemented in [38]. But the employed optimization algorithm is the conventional PSO, which has the drawback of getting converged to the local optima [12]. Therefore in this work new and improved MWOA is employed for better training of the SNN. The objective functions for the MWOA based optimization are as mentioned in equations 8 and 9 respectively. The Figure 22 (a and b) shows the basic idea of the proposed work, in which the weights from the SNN are fed to the MWOA optimization environment. The MWOA based training of SNN starts by random initialization of search agents of MWOA and hyper-parameters (U^{SE}, τ^m, τ^{rec}) of SNN. In addition to that, to begin the algorithmic training of SNN, it is important to consider certain fixed values for the parameter such as Decay time constant= 10 ms, threshold membrane potential = 7 mV, reset voltage = 0.05 mV, population size = 50, iterations = 160, runs = 30 and η^m=20. The detailed working of the MWOA training of the SNN is as explained in points 1-12 under the section IV(C). The optimization search space is formed based on the fitness function $\varepsilon = \frac{1}{2}\sum_{o=1}^{o'}(t_a^o - t_d^o)$ which is inturn dependent on the timing of the spike train. Here the actual and the desired spike timing is dependent on equations 8 and 9 respectively [54]. The optimization process starts with the random initialization of the search agents in the search space. At the beginning of the iteration search agents explore the search space and as the iteration proceeds, the search agents converge towards the best solution as shown in Figure 22 (a). After each iteration best search agent is selected based on its fitness value. As the iterations progresses search agents exhibits mutation and expert balance between its exploration and exploitation ability to exercise a better exploitative search. At the end of maximum iteration, the best solutions i.e optimized weight values of SNN for minimized value of the fitness function are retrieved. The pseudocode for the detailed working of the MWOA based optimization of the SNN weights are discussed in the Algorithm 1.

Algorithm 1 Pseudocode for MWOA

Random initialization of the whales/search agents, $\vec{X}$,wˆij˙m *weight values as in Eq. 6*
Obtain the values of a,A (via Eq.(26)) and C
Compute finess value of each search agents for the fitness function:$x^j(t) = \sum_i \sum_{m=1}^{K} \mathrm{Y}_m^i w_m^{ij}$
Random initialization of p
While $n < n_{max}$
if $p \leq 0.5$ and $|A| \leq 1$
  Search agents' position gets updated based on Eqs.(24) and (25)
else if $p > 0.5$ *and* $|A| \leq 1$
  Search agents' position gets updated based on the Eq.(27)
end
Compute d˙1 and d˙2 as per Eq.(31) and Eq.(32)
if $d_1 < d_2$ *and* $p \leq 0.5$ *and* $|A| \leq 1$
  Search agents' position gets updated based on the Eq.(34)
end
Perform Mutation and Replacement based on Eqs.(35-37)
Check for the boundary of search space and constraints
Compute search agents' fitness based on the fitness function in $\varepsilon = \frac{1}{2}\sum_{o=1}^{o'}(t_a^o - t_d^o)$
Compute the best solution and update it
n=n+1
end while
Best Solution=$X*$

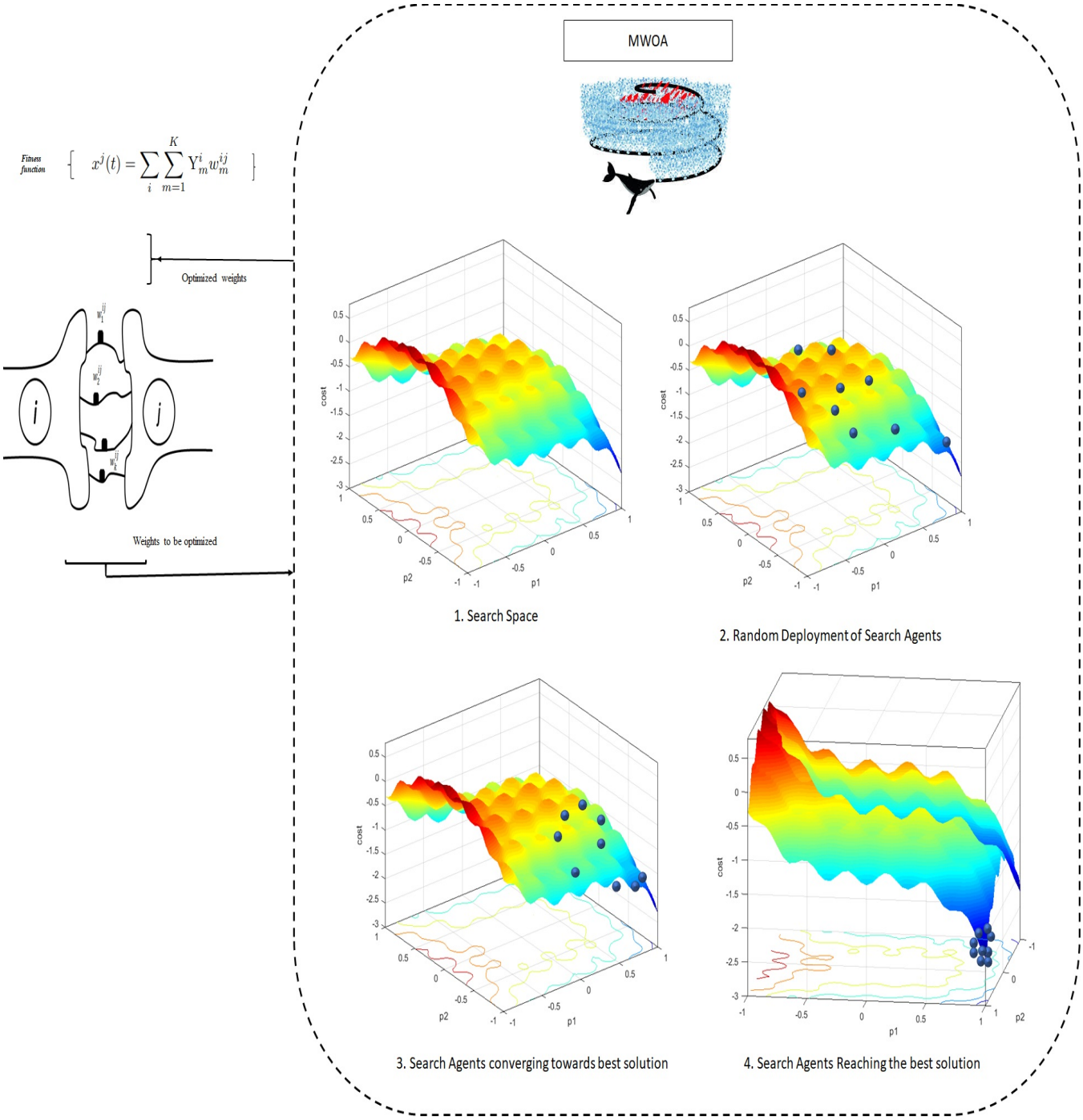

Fig. 22: Working of the proposed MWOA optimization of SNN during convergence

8 Simulation Results

In this paper, the objective functions in Eq.(8) and Eq.(9) are optimized to improve the efficiency of SNN. An efficiently trained neural network is identified by its high accuracy in classification during testing and training. The training of SNN is carried out in MATLAB 2020(a) based simulation environment. The CWT of the PU signal obtained via USRPs N210 is performed in the MATLAB 2020(a). To obtain the real time signals via USRPs the software platforms employed are LabVIEW 2018, GNU Radio Companion 3.7.11 and MATLAB 2020(a) in the Ubuntu 18.04.

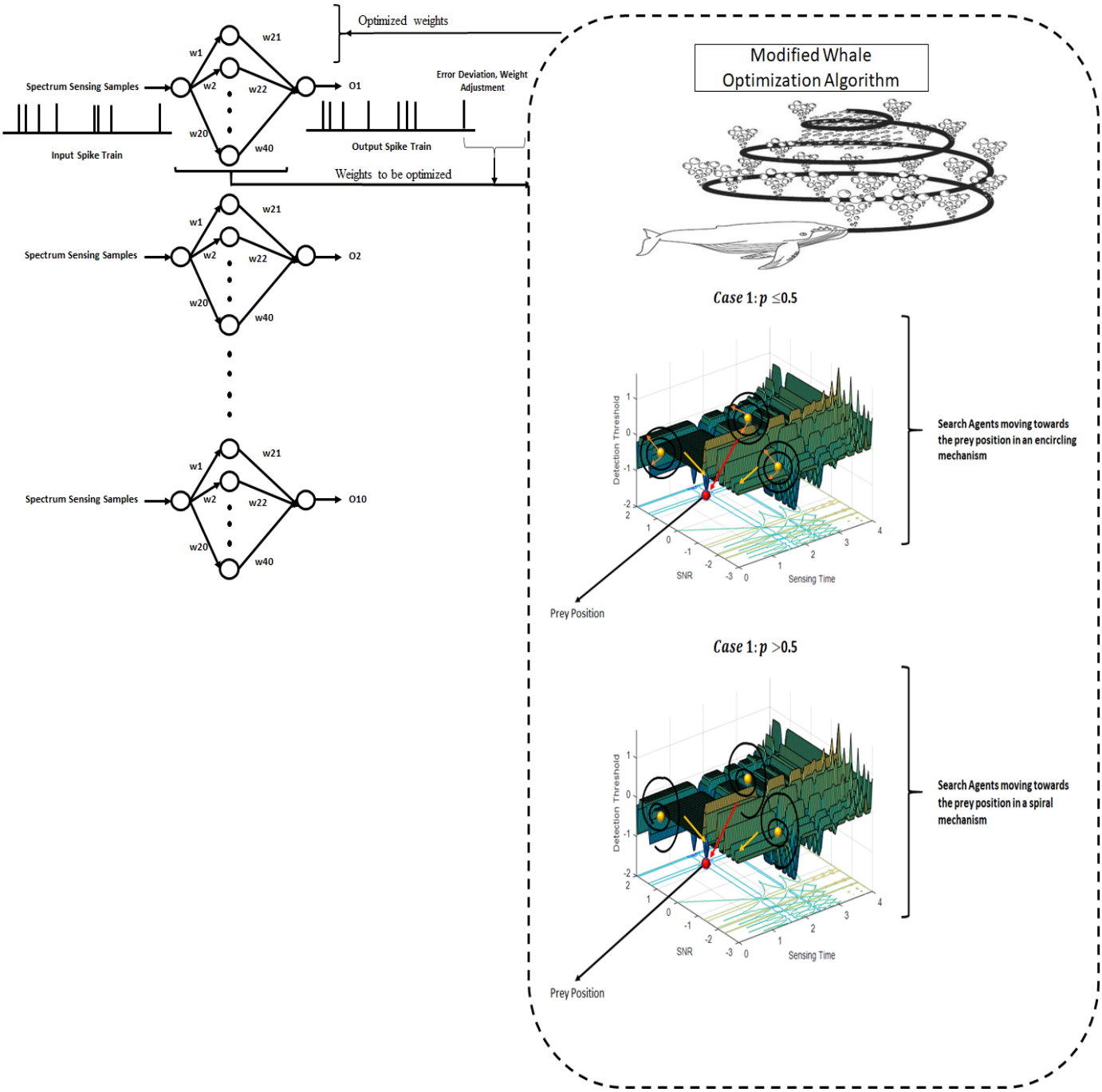

Fig. 23: Working of the proposed MWOA optimization of SNN during initialization

The proposed Mutated MWOA-SNN based spectrum sensing is compared with PSO, PSOGSA, GSA and ASA. The comparison is made in terms of convergence curve for training accuracy, the opportunistic throughput and the BER for the relay based scenario. The parameters considered for simulation are: The number of CR_s=5, σ=$[0.08, 0.08, 0.08, 0.08, 0.08]^T$ (noise variance), v (control channel noise variance)=$[0.08, 0.08, 0.08, 0.08, 0.08]^T$, $N_0 = 1 \times 10^{-6}$ W/Hz. Transmission power associated with PU BS lies in a range 25 dBm to 45 dBm, the power associated with the CR-FC transmission is between 20 dBm and 30 dBm [11]. The power of each UE is considered to be limited to 0.1 W. The channel gains $h_{j,k,t}^{B,CRFC}$, $h_{j,k,t}^{CRFC,UE}$ and $h_{j,k,t}^{UE,CRFC}$, $h_{j,k,t}^{CRFC,B}$ are Rayleigh faded channel.

The channel between LU and CRs is considered to be independent of the channels $h_{j,k,t}^{B,CRFC}, h_{j,k,t}^{CRFC,UE}$ and $h_{j,k,t}^{UE,CRFC}, h_{j,k,t}^{CRFC,B}$. The α=11.9, β=0.14, J_1=10.39, J_2=0.05, G_1=29.06, G_2=0.03, d_o reference distance=1 m, Υ_1=3 dB, Υ_2=23 dB [20]. The population size of search agents/whales/particles = 50. Each employed optimization scheme is iterated for 30 runs with each run corresponds to the 160 iterations for training the SNN. The rationale on the choice of the parameters and mentioning only the key parameters in Table 2 is because of their greater influence on the training of SNN in terms of reaching the optimal values of the weights. We have experimented with different set of values and the values for which optimum weights can be achieved are mentioned in Table 2.

TABLE 2: Simulation Parameter values

Parameter	Values
α	11.9
β	0.14
J_1	10.39
J_2	0.05
G_1	29.06
G_2	0.03
d_o reference distance	1m
Υ_1	3dB
Υ_2	23dB
h	30m
h_{BS}	20m
No. of CR_s	5
Threshold Membrane Potential	7 mV
Reset Voltage	0.05 mV
Search agent population size	50
PSO and PSOGSA cognitive and social parameter constants	2
PSO and PSOGSA inertia weight	Random number between [0,1]
GSA and PSOGSA gravitational constant	1
Transmitter USRP	Ettus N210
Receiver USRP	Ettus B210

Figures 24-30 show the training accuracy for the Conventional SNN, GSA trained SNN, PSO trained SNN, PSOGSA trained SNN, ASA trained SNN and the proposed mutated MWOA trained SNN. Here blue solid line represent the accuracy and the black dashed line represents the loss obtained during the training phase. The loss infers the validation accuracy during the training of each algorithm. The reason for displaying the training accuracy and the loss is to show the training efficiency of each algorithm. The conventional SNN achieved an accuracy of 52% during the training phase. Whereas PSO trained SNN and GSA trained SNN has the validation accuracy (represented in black dash line) of 58% and 55% respectively. The PSOGSA trained SNN achieved an accuracy of about 60%. The ASA trained SNN performed well and attained the accuracy of 90%. The proposed mutated MWOA because of its efficient ability to overcome local optima and execute the training of SNN by guiding the weight values towards the global best achieved the validation accuracy of 96.88%.

The efficient performance of the proposed MWOA in training SNN is because the proposed scheme is successful in maintaining the efficient balance between its exploration and exploitation abilities. The MWOA has good approach of avoiding local optima solution by effectively mutating the search agents and replacing the worst solution. In this way the algorithm move towards the global best solution. The high training accuracy values so obtained using MWOA-SNN is visible in its performance in efficiently detecting the spectrum holes and utilizing it for data transmission. Figures 30 and 31 depicts the performance of the proposed scheme in transferring data between UE and BS (vice-versa) via utilizing the efficiently detected spectrum holes. The performance is indexed in terms of opportunistic throughput for varying SNR. The proposed MWOA-SNN has achieved higher opportunistic throughput for the sensing time of 3 ms and

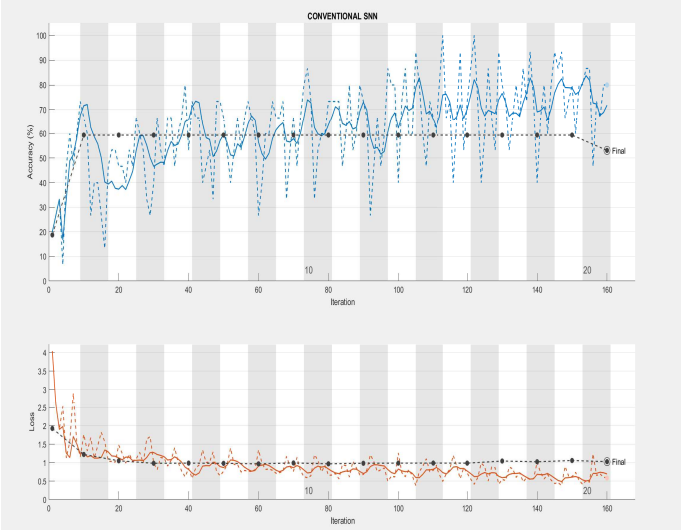

Fig. 24: Convergence Curve for the Accuracy and the Loss for the Conventional SNN

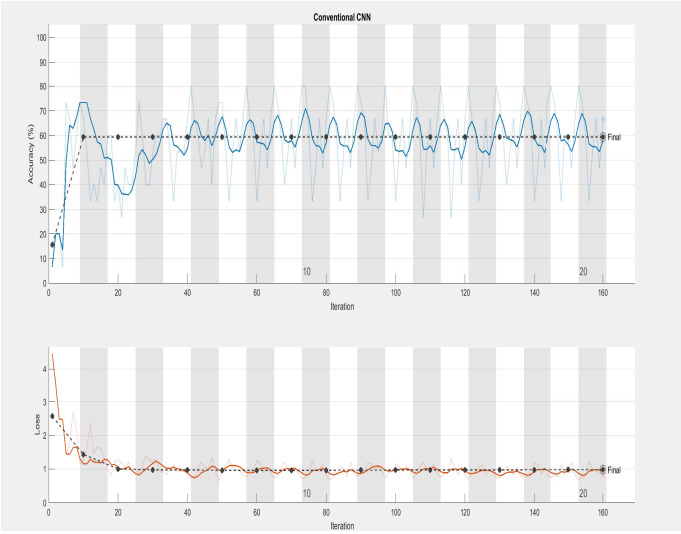

Fig. 25: Convergence Curve for the Accuracy and the Loss for the Conventional CNN

frame period 50 as compared to ASA-SNN, PSO-SNN, GSA-SNN and PSOGSA-SNN based spectrum sensing.

The optimized weights obtained via proposed MWOA is employed to train the SNN. The trained SNN is tested for the real time scenario by performing spectrum sensing using USRPs N210. The test bench setup is as shown in figures 33 and 34. The USRP 1 act as a primary transmitter transmitting at certain intervals. The USRP 2 performs spectrum sensing and detects the vacant spectrum based on the MWOA trained SNN. The spectrum is vacant when PU is not transmitting. Utilizing the spectrum holes the USRP 1 then transfers data to the Receiver USRP (B210).

The testing results so obtained for the trained SNN in the real time scenario is as shown in Figure 35. The accuracy achieved in testing period/working phase for mutated MWOA-SNN is compared with the ASA, PSO, PSOGSA, GSA, and conventional SNN.

Figure 35 displays the validation accuracy of each algorithm during the working phase. It can be infered that with less time computation, mutated MWOA trained SNN is able to correctly distinguish the presence and the absence of the PU. The Accuracy of MWOA trained SNN based Cognitive radio network is better as compared to PSO, PSOGSA, GSA, and Conventional SNN. The performance of MWOA in effectively

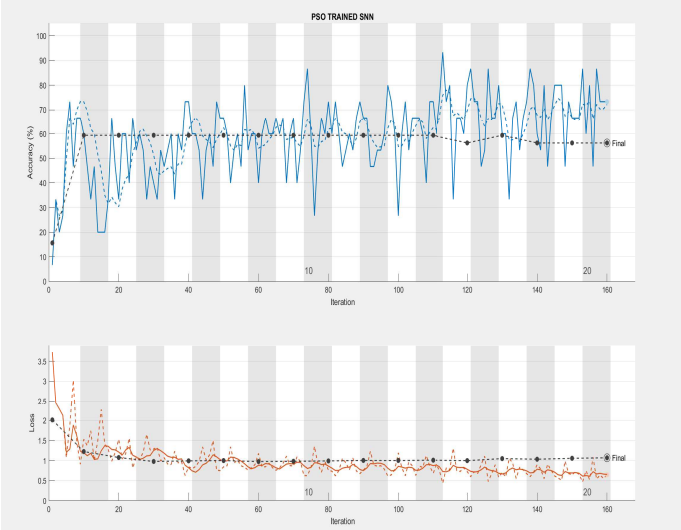

Fig. 26: Convergence Curve for the Accuracy and the Loss for the PSO trained SNN

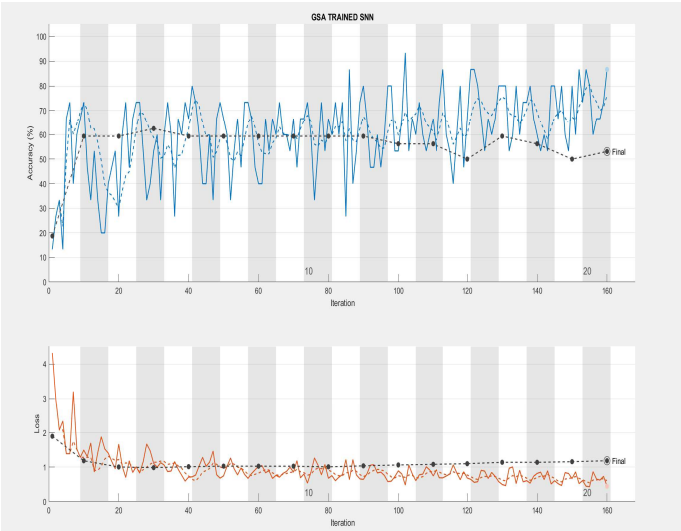

Fig. 27: Convergence Curve for the Accuracy and the Loss for the GSA trained SNN

detecting the spectrum holes is justified by the BER performance as shown in Figure 37. The efficient mutation and expert exploration scheme have efficiently enhanced the performance of the MWOA and as result the presence and the absence of the PU is correctly detected and data is transmitted with less error.

9 Result Analysis

Figures 24 and 25 show the training and validation accuracy achieved via conventional SNN and conventional CNN. It can be seen that the conventional SNN has better training and validation accuracy as compared to conventional CNN. Thus showing the effectiveness of SNN in classifying the presence and absence of the PU signal. But still the obtained accuracy is not able to approach 100 percent accuracy. This shows that both the conventional CNN and SNN are able to classify the signal but are not efficient enough to be employed for spectrum sensing. Therefore, in this work novel MWOA training scheme is employed for SNN to enhance its efficiency while training. The effectiveness of the proposed MWOA in training the SNN to correctly identify the spectrum holes can be inferred via high opportunistic throughput achieved in figures 31-32 and PU detection and BER performance in figures 36-37. Post weight optimization of

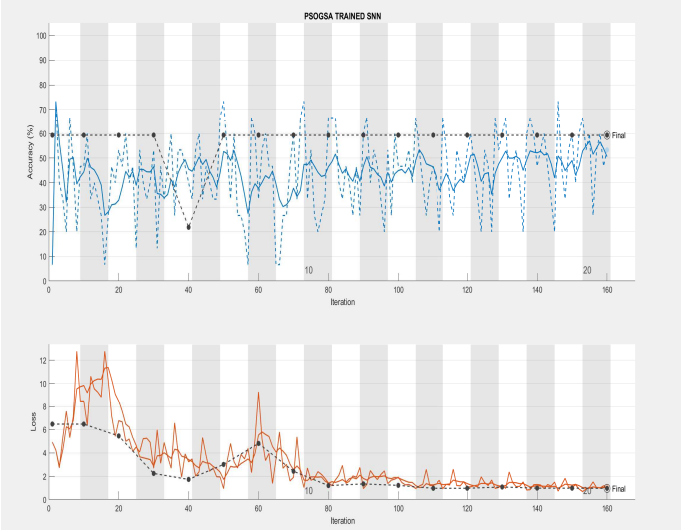

Fig. 28: Convergence Curve for the Accuracy and the Loss for the PSOGSA trained SNN

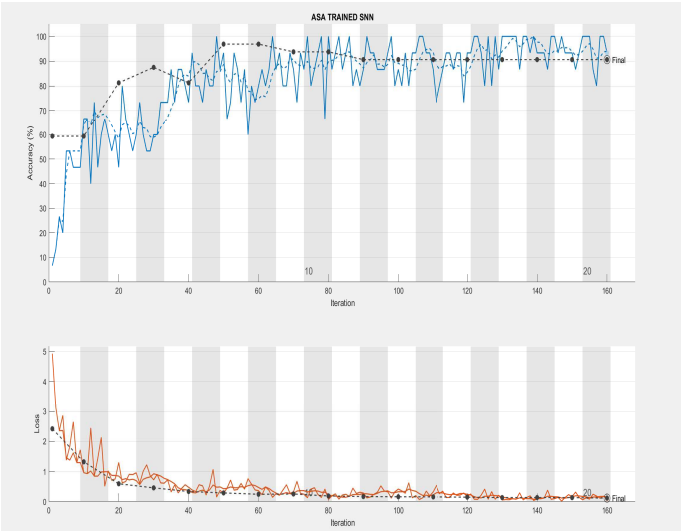

Fig. 29: Convergence Curve for the Accuracy and the Loss for the ASA trained SNN

SNN,The proposed MWOA-SNN is employed in real time spectrum sensing via USRPs. Figures 31 and 32 show that opportunistic throughput achieved for MWOA trained SNN is the highest. The MWOA because of its novel mutation abilities is capable to optimize the weights of SNN. Therefore, MWOA-SNN is more capable to correctly identify and classify the vacant channel as compared to conventional SNN and other metaheuristic trained SNN. The proposed MWOA optimization has efficiently improved the classification ability of the conventional SNN. Thus, the proposed MWOA-SNN is successfully implemented for efficient spectrum sensing in CR networks. Tables 3 and 4 show the comparative analysis of the optimization algorithms employed for training SNN in terms of opportunistic throughput. The mutated MWOA has clearly outperformed ASA, PSOGSA, PSO and GSA algorithms in efficiently training the SNN to correctly identify the spectrum holes. Thus, improving the opportunistic throughput. The Table 5 shows that the proposed MWOA trained SNN is quick enough to obtain the desirable validation accuracy. Thus, making it a good fit for implementing in the real time scenario.

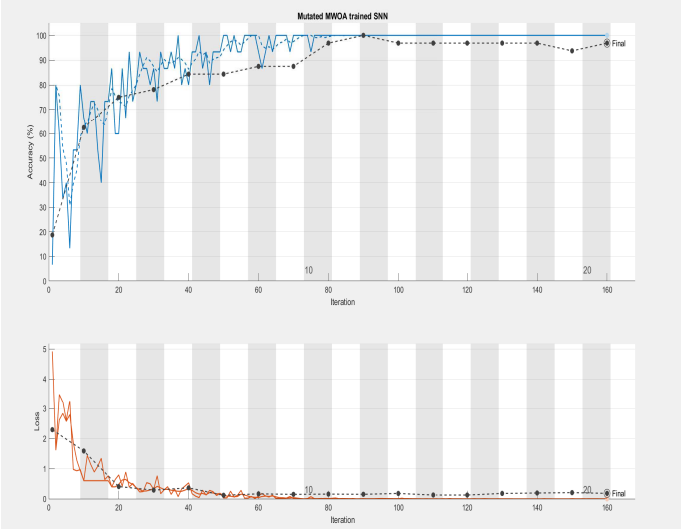

Fig. 30: Convergence Curve for the Accuracy and the Loss for the proposed mutated MWOA trained SNN

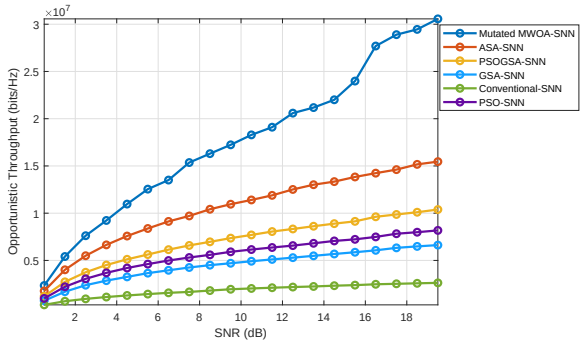

Fig. 31: Opportunistic Throughput vs SNR (For UE to BS)

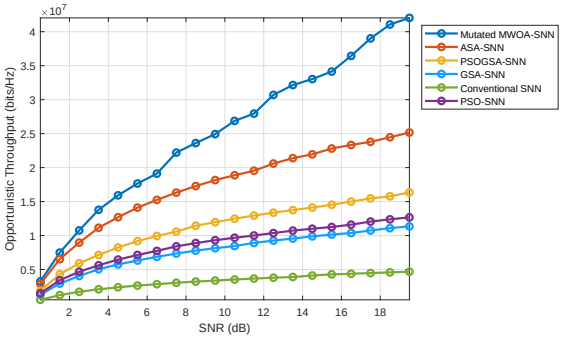

Fig. 32: Opportunistic Throughput vs SNR (For BS to UE)

TABLE 3: Opportunistic Throughput For UE to BS at SNR= 20 dB

Optimization Algorithm	Mutated MWOA	ASA	PSOGSA	PSO	GSA	Conventional SNN
Opportunistic Throughput (bits/Hz)	$3x10^7$	$1.5x10^7$	$1x10^7$	$0.75x10^7$	$0.65x10^7$	$0.25x10^7$

TABLE 4: Opportunistic Throughput For BS to UE at SNR= 20 dB

Optimization Algorithm	Mutated MWOA	ASA	PSOGSA	PSO	GSA	Conventional SNN
Opportunistic Throughput (bits/Hz)	$4.2x10^7$	$2.5x10^7$	$1.62x10^7$	$1.46x10^7$	$1.3x10^7$	$0.5x10^7$

TABLE 5: Validation Accuracy achieved during testing period at 0.02 seconds

Optimization Algorithm	Mutated MWOA	ASA	PSOGSA	PSO	GSA	Conventional SNN
Accuracy Percentage	98	96	88	82	82	80

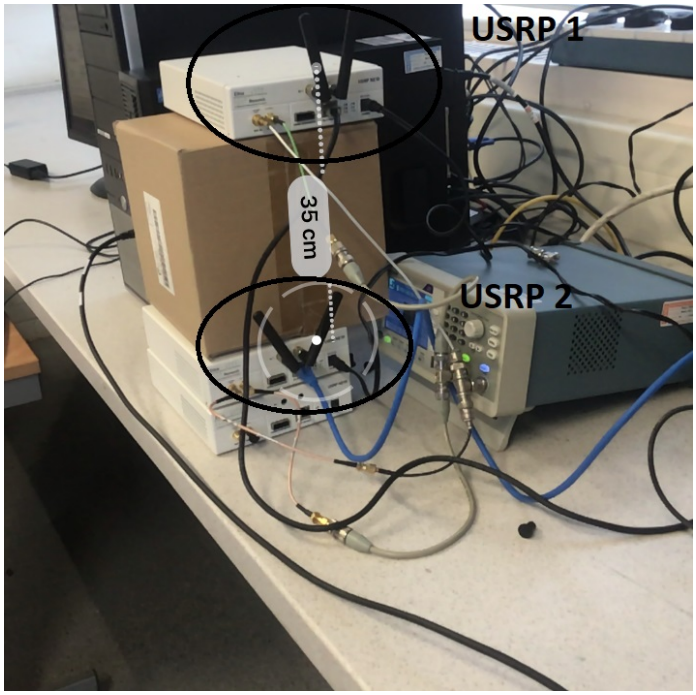

Fig. 33: Test bench setup Transmitter

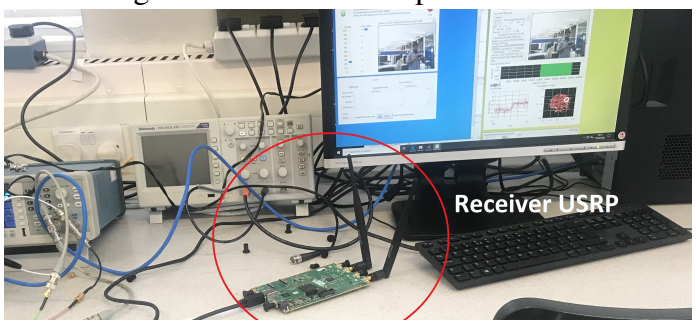

Fig. 34: Test bench setup Receiver

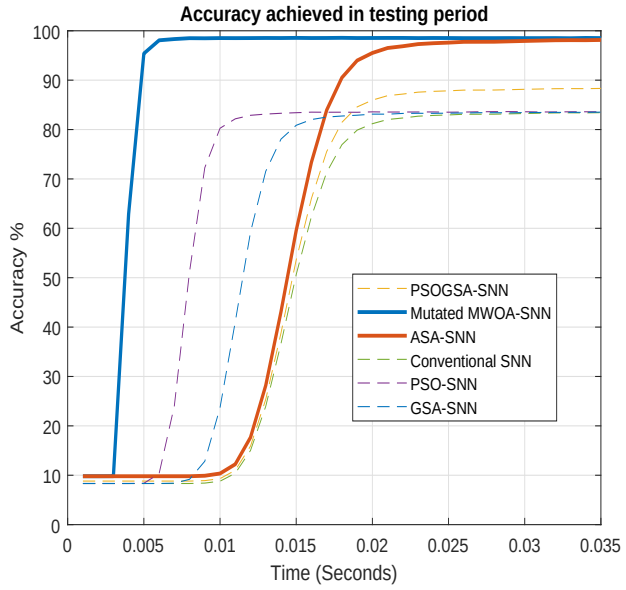

Fig. 35: Validation accuracy comparison for the testing period

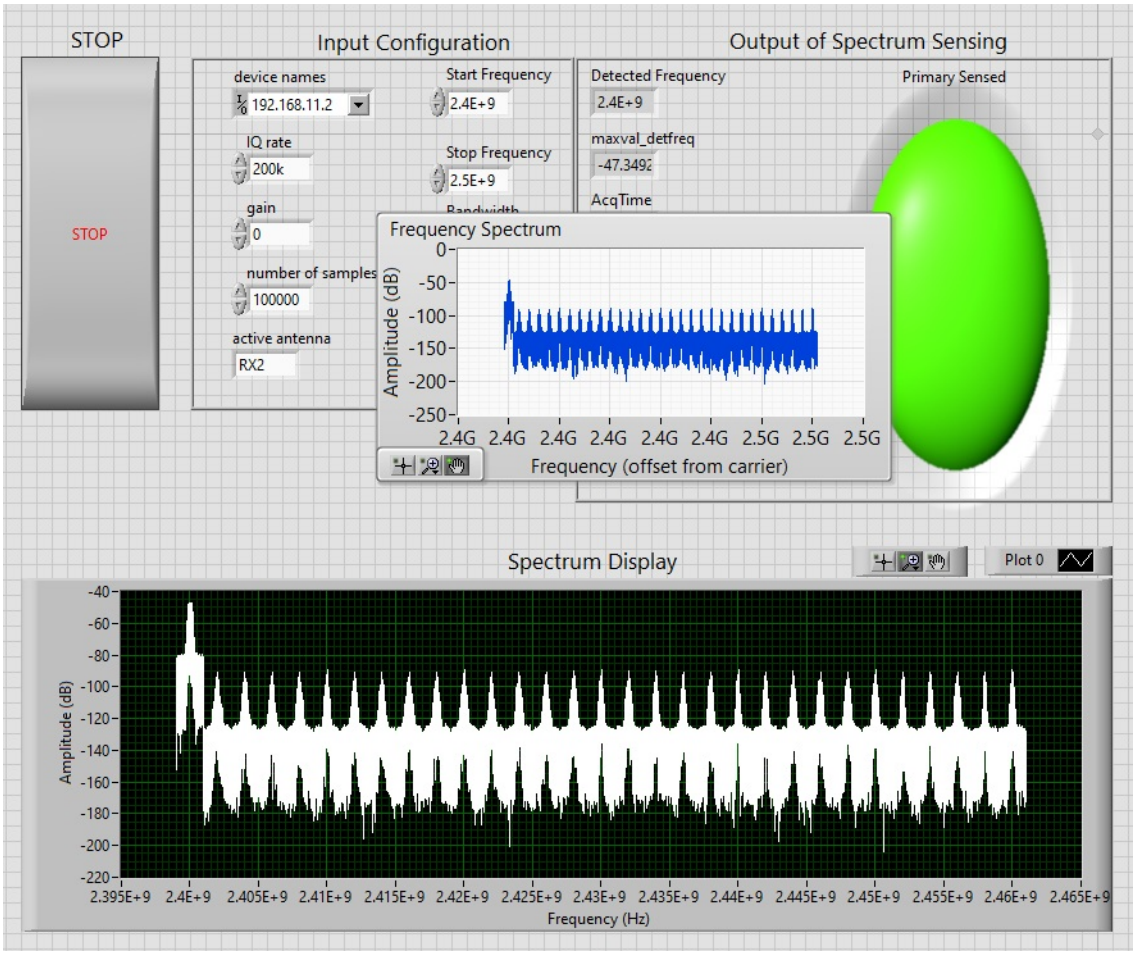

Fig. 36: PU detected at 2.4 GHz using NI LabVIEW and the proposed scheme

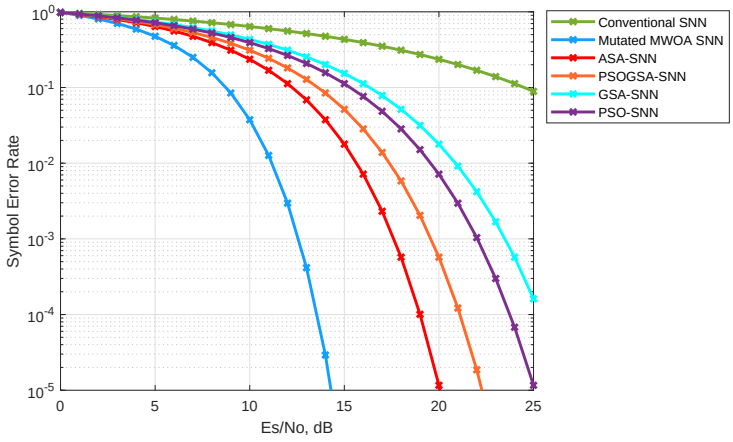

Fig. 37: BER vs SNR

10 CONCLUSION

In this paper, a new training algorithm MWOA is proposed and implemented for SNN based efficient spectrum sensing in CR relay network. The employed scheme successfully overcomes the issue of network coverage and spectrum congestion simultaneously by improving the opportunistic throughput and the BER performance of the CR relay network. The proposed MWOA is effective in enhancing the classification abilities of the conventional SNN with an 18% improvement in the validation accuracy of MWOA-SNN compared to conventional SNN during the testing period. The MWOA trained SNN increases the efficiency of the cognitive radio network. The MWOA trained SNN is implemented for offline spectrum sensing, in which SNN is first trained using MWOA and the trained network is then employed for detecting the vacant spectrum. The simulation results show the efficacy of the proposed MWOA in enhancing the classification ability of the SNN and thus improving the spectrum sensing scheme. The Mutated MWOA training of SNN achieved the validation accuracy of 98% as compared to the 80%, 82%, 82%, 88%, and 96% for the Conventional SNN, PSO-SNN, GSA-SNN, PSOGSA-SNN and ASA-SNN respectively. The proposed MWOA trained SNN is then employed for the real time spectrum sensing for the sensing time of 3 ms and frame period 50 ms via USRP N210 and B210. The proposed scheme efficiently detected the presence and the absence of PU transmission at 2.4 GHz.

REFERENCES

[1] Choi, Y., Ji, H. W., Park, J. Y., Kim, H. C., and Silvester, J. A. (2011). A 3W network strategy for mobile data traffic offloading. IEEE Communications Magazine, 49(10), 118-123. DOI:10.1109/MCOM.2011.6035825

[2] Rosnes, E., and Ytrehus, Y. (2005). Improved algorithms for the determination of turbo-code weight distributions. IEEE Transactions on communications, 53(1), 20-26. DOI:10.1109/TCOMM.2004.840632

[3] Naguib, A. F., Tarokh, V., Seshadri, N., and Calderbank, A. R. (1998). A space-time coding modem for high-data-rate wireless communications. IEEE Journal on Selected areas in Communications, 16(8), 1459-1478. DOI:10.1109/49.730454

[4] Tarokh, V., Seshadri, N., and Calderbank, A. R. (1998). Space-time codes for high data rate wireless communication: Performance criterion and code construction. IEEE transactions on information theory, 44(2), 744-765. DOI:10.1109/18.661517

[5] Xiang, W., Zheng, K., and Shen, X. S. (Eds.). (2016). 5G mobile communications. Springer.

[6] Yucek, T., and Arslan, H. (2009). A survey of spectrum sensing algorithms for cognitive radio applications. IEEE communications surveys and tutorials, 11(1), 116-130. DOI:10.1109/SURV.2009.090109

[7] Berger, S., Kuhn, M., Wittneben, A., Unger, T., and Klein, A. (2009). Recent advances in amplify-and-forward two-hop relaying. IEEE Communications Magazine, 47(7), 50-56. DOI:10.1109/MCOM.2009.5183472

[8] Quan, Z., Cui, S., and Sayed, A. H. (2008). Optimal linear cooperation for spectrum sensing in cognitive radio networks. IEEE Journal of selected topics in signal processing, 2(1), 28-40. DOI:10.1109/JSTSP.2007.914882

[9] Rashid, R. A., Hamid, A. H. F. B. A., Fisal, N., Syed-Yusof, S. K., Hosseini, H., Lo, A., and Farzamnia, A. (2015). Efficient in-band spectrum sensing using swarm intelligence for cognitive radio network. Canadian Journal of Electrical and Computer Engineering, 38(2), 106-115. DOI:10.1109/CJECE.2014.2378258

[10] Mirjalili, S., and Lewis, A. (2016). The whale optimization algorithm. Advances in engineering software, 95, 51-67. https://doi.org/10.1016/j.advengsoft.2016.01.008

[11] Dahlman, E., Parkvall, S., Skold, J., and Beming, P. (2010). 3G evolution: HSPA and LTE for mobile broadband. Academic press.

[12] Eappen, G., and Shankar, T. (2020). Hybrid PSO-GSA for energy efficient spectrum sensing in cognitive radio network. Physical Communication, 101091. https://doi.org/10.1016/j.phycom.2020.101091

[13] Venugopal, K., Valenti, M. C., and Heath, R. W. (2016). Device-to-device millimeter wave communications: Interference, coverage, rate, and finite topologies. IEEE Transactions on Wireless Communications, 15(9), 6175-6188. DOI:10.1109/TWC.2016.2580510

[14] Balanis, C. A. (2016). Antenna theory: analysis and design. John wiley and sons.

[15] Mondal, B., Thomas, T. A., Visotsky, E., Vook, F. W., Ghosh, A., Nam, Y. H., ... and Kakishima, Y. (2015). 3D channel model in 3GPP. IEEE Communications Magazine, 53(3), 16-23. DOI:10.1109/MCOM.2015.7060514

[16] Al-Hourani, A., Kandeepan, S., and Jamalipour, A. (2014, December). Modeling air-to-ground path loss for low altitude platforms in urban environments. In 2014 IEEE global communications conference (pp. 2898-2904). IEEE. DOI:10.1109/GLOCOM.2014.7037248

[17] Mozaffari, M., Saad, W., Bennis, M., Nam, Y. H., and Debbah, M. (2019). A tutorial on UAVs for wireless networks: Applications, challenges, and open problems. IEEE communications surveys and tutorials, 21(3), 2334-2360. DOI:10.1109/COMST.2019.2902862

[18] Mozaffari, M., Saad, W., Bennis, M., and Debbah, M. (2016). Unmanned aerial vehicle with underlaid device-to-device communications: Performance and tradeoffs. IEEE Transactions on Wireless Communications, 15(6), 3949-3963. DOI:10.1109/TWC.2016.2531652

[19] Talbi, E. G. (2009). Metaheuristics: from design to implementation (Vol. 74). John Wiley and Sons.

[20] Mozaffari, M. (2018). Wireless Communications and Networking with Unmanned Aerial Vehicles: Fundamentals, Deployment, and Optimization (Doctoral dissertation, Virginia Tech). http://hdl.handle.net/10919/83921

[21] Asadi, A., Wang, Q., and Mancuso, V. (2014). A survey on device-to-device communication in cellular networks. IEEE Communications Surveys and Tutorials, 16(4), 1801-1819. DOI:10.1109/COMST.2014.2319555

[22] Li, P., and Guo, S. (2014). Cooperative device-to-device communication in cognitive radio cellular networks. Springer International Publishing. DOI:10.1007/978-3-319-12595-4

[23] Sultana, A., Zhao, L., and Fernando, X. (2017). Efficient resource allocation in device-to-device communication using cognitive radio technology. IEEE Transactions on Vehicular Technology, 66(11), 10024-10034. DOI:10.1109/TVT.2017.2743058
[24] Zheng, S., Lou, C., and Yang, X. (2010). Cooperative spectrum sensing using particle swarm optimisation. Electronics letters, 46(22), 1525-1526. DOI:10.1049/el.2010.2115
[25] Rashid, R. A., Hamid, A. H. F. B. A., Fisal, N., Syed-Yusof, S. K., Hosseini, H., Lo, A., and Farzamnia, A. (2015). Efficient in-band spectrum sensing using swarm intelligence for cognitive radio network. Canadian Journal of Electrical and Computer Engineering, 38(2), 106-115. DOI:10.1109/CJECE.2014.2378258
[26] Das, D., and Das, S. (2014, February). A cooperative spectrum sensing scheme using multiobjective hybrid IWO/PSO algorithm in cognitive radio networks. In 2014 International Conference on Issues and Challenges in Intelligent Computing Techniques (ICICT) (pp. 225-230). IEEE. DOI:10.1109/MICC.2015.7725407
[27] Eappen, G., and Shankar, T. (2018). Energy efficient spectrum sensing for cognitive radio network using artificial bee colony algorithm. International Journal of Engineering and Technology, 7(4), 2319-2324. DOI:10.14419/ijet.v7i4.10094
[28] Yang, X. S. (2014). Swarm intelligence based algorithms: a critical analysis. Evolutionary intelligence, 7(1), 17-28. DOI:10.1007/s12065-013-0102-2
[29] Tang, Y. J., Zhang, Q. Y., and Lin, W. (2010, September). Artificial neural network based spectrum sensing method for cognitive radio. In 2010 6th International Conference on Wireless Communications Networking and Mobile Computing (WiCOM) (pp. 1-4). IEEE. DOI:10.1109/WICOM.2010.5601105Co
[30] Zhang, M., Diao, M., and Guo, L. (2017). Convolutional neural networks for automatic cognitive radio waveform recognition. IEEE Access, 5, 11074-11082. DOI:10.1109/ACCESS.2017.2716191
[31] Kartalopoulos, S. V., and Kartakapoulos, S. V. (1997). Understanding neural networks and fuzzy logic: basic concepts and applications. Wiley-IEEE Press.
[32] Wade, J. J., McDaid, L. J., Santos, J. A., and Sayers, H. M. (2010). SWAT: a spiking neural network training algorithm for classification problems. IEEE Transactions on Neural Networks, 21(11), 1817-1830. DOI:10.1109/TNN.2010.2074212
[33] Qi, Y., Shen, J., Wang, Y., Tang, H., Yu, H., Wu, Z., and Pan, G. (2018, July). Jointly Learning Network Connections and Link Weights in Spiking Neural Networks. In IJCAI (pp. 1597-1603). DOI:10.24963/ijcai.2018/221
[34] Hebb, D. O. (1949). The organization of behavior: a neuropsychological theory. J. Wiley; Chapman and Hall.
[35] Chen, M., Challita, U., Saad, W., Yin, C., and Debbah, M. (2017). Machine learning for wireless networks with artificial intelligence: A tutorial on neural networks. arXiv preprint arXiv:1710.02913, 9. Corpus ID: 26853250
[36] Stimberg, M., Brette, R., and Goodman, D. F. (2019). Brian 2, an intuitive and efficient neural simulator. Elife, 8, e47314. DOI: 10.7554/eLife.47314
[37] Brunel, N., and Latham, P. E. (2003). Firing rate of the noisy quadratic integrate-and-fire neuron. Neural Computation, 15(10), 2281-2306. doi: 10.1162/089976603322362365.
[38] Mohemmed, A., Matsuda, S., Schliebs, S., Dhoble, K., and Kasabov, N. (2011, July). Optimization of spiking neural networks with dynamic synapses for spike sequence generation using PSO. In The 2011 International Joint Conference on Neural Networks (pp. 2969-2974). IEEE. DOI:10.1109/IJCNN.2011.6033611
[39] Sichtig, H. (2007, April). Building Smart Machines by Utilizing Spiking Neural Networks; Current Perspectives. In 2007 IEEE Symposium on Computational Intelligence and Bioinformatics and Computational Biology (pp. 346-350). IEEE. DOI:10.1109/CIBCB.2007.4221243
[40] S. M. Bohte and J. N. Kok. Applications of spiking neural networks. In Process. Lett., 95:519-520, September 2005.
[41] Belatreche, A., Maguire, L. P., and McGinnity, M. (2007). Advances in design and application of spiking neural networks. Soft Computing, 11(3), 239-248. DOI:10.1007/s00500-006-0065-7
[42] Namarvar, H. H., Liaw, J. S., and Berger, T. W. (2001, July). A new dynamic synapse neural network for speech recognition. In IJCNN'01. International Joint Conference on Neural Networks. Proceedings (Cat. No. 01CH37222) (Vol. 4, pp. 2985-2990). IEEE. DOI:10.1109/IJCNN.2001.938853
[43] Pavlidis, N. G., Tasoulis, O. K., Plagianakos, V. P., Nikiforidis, G., and Vrahatis, M. N. (2005, July). Spiking neural network training using evolutionary algorithms. In Proceedings. 2005 IEEE International Joint Conference on Neural Networks, 2005. (Vol. 4, pp. 2190-2194). IEEE. DOI:10.1109/IJCNN.2005.1556240
[44] Bohte, S. M., Kok, J. N., and La Poutre, H. (2002). Error-backpropagation in temporally encoded networks of spiking neurons. Neurocomputing, 48(1-4), 17-37. https://doi.org/10.1016/S0925-2312(01)00658-0
[45] Pfister, J. P., Barber, D., and Gerstner, W. (2003). Optimal hebbian learning: A probabilistic point of view. In Artificial Neural Networks and Neural Information Processing-ICANN/ICONIP 2003 (pp. 92-98). Springer, Berlin, Heidelberg.
[46] Eappen, G., and Shankar, T. (2020). A Survey on Soft Computing Techniques for Spectrum Sensing in a Cognitive Radio Network. SN Computer Science, 1(6), 1-36. DOI:10.1007/s42979-020-00372-z
[47] Hebb, D. O. (1949). The organization of behavior: a neuropsychological theory. J. Wiley; Chapman and Hall.
[48] Liaw, J. S., and Berger, T. W. (1999). Dynamic synapse: Harnessing the computing power of synaptic dynamics. Neurocomputing, 26, 199-206. DOI:10.1016/S0925-2312(99)00063-6
[49] Maass, W., and Zador, A. (1999). Computing and learning with dynamic synapses. Pulsed neural networks, 6(May), 321-336.
[50] Tsodyks, M., Pawelzik, K., and Markram, H. (1998). Neural networks with dynamic synapses. Neural computation, 10(4), 821-835. DOI:10.1162/089976698300017502
[51] Thomson, A. M., and Deuchars, J. (1994). Temporal and spatial properties of local circuits in neocortex. Trends in neurosciences, 17(3), 119-126. https://doi.org/10.1016/0166-2236(94)90121-X
[52] Willis, P., Gobinddass, M. L., Garayt, B., and Fagard, H. (2012). Recent Improvements in DORIS Data Processing at IGN in View of ITRF2008, the ignwd08 Solution. In Geodesy for Planet Earth (pp. 43-49). Springer, Berlin, Heidelberg.
[53] Paiva, A. R., Park, I., and PrÃncipe, J. C. (2010). A comparison of binless spike train measures. Neural Computing and Applications, 19(3), 405-419. https://doi.org/10.1007/s00521-009-0307-6

[54] Kulkarni, S., Simon, S. P., and Sundareswaran, K. (2013). A spiking neural network (SNN) forecast engine for short-term electrical load forecasting. Applied Soft Computing, 13(8), 3628-3635. https://doi.org/10.1016/j.asoc.2013.04.007
[55] Imris, P. (2006). Transient based earth fault location in 110 kV subtransmission networks. Helsinki University of Technology.
[56] Robertson, D. C., Camps, O. I., Mayer, J. S., and Gish, W. B. (1996). Wavelets and electromagnetic power system transients. IEEE Transactions on Power Delivery, 11(2), 1050-1058. https://doi.org/10.1109/61.489367
[57] Eappen, G., Shankar, T., and Nilavalan, R. (2020, September). Efficient Spectrum Sensing for the Relay Based Cognitive Radio Network for Enhancing the Network Coverage for Wireless Patient Monitoring System. In 2020 5th International Conference on Smart and Sustainable Technologies (SpliTech) (pp. 1-6). IEEE. DOI: 10.23919/SpliTech49282.2020.9243745
[58] Eappen, G., Shankar, T. Multi-Objective Modified Grey Wolf Optimization Algorithm for Efficient Spectrum Sensing in the Cognitive Radio Network. Arab J Sci Eng (2020). https://doi.org/10.1007/s13369-020-05084-3
[59] Stimberg, M., Brette, R., and Goodman, D. F. (2019). Brian 2, an intuitive and efficient neural simulator. Elife, 8, e47314. doi: 10.7554/eLife.47314
[60] Ghany, K. K. A., AbdelAziz, A. M., Soliman, T. H. A., and Sewisy, A. A. E. M. (2020). A hybrid modified step whale optimization algorithm with Tabu search for data clustering. Journal of King Saud University-Computer and Information Sciences. DOI:10.1016/j.jksuci.2020.01.015
[61] Eappen, G., Shankar, T., and Nilavalan, R. (2021). Advanced squirrel algorithm trained neural network for efficient spectrum sensing in cognitive radio based air traffic control application. IET Communications. https://doi.org/10.1049/cmu2.12111
[62] Yang, H., Wang, B., Yao, Q., Yu, A., and Zhang, J. (2019). Efficient hybrid multi-faults location based on hopfield neural network in 5G coexisting radio and optical wireless networks. IEEE Transactions on Cognitive Communications and Networking, 5(4), 1218-1228. DOI:10.1109/TCCN.2019.2946312
[63] Yang, H., Yao, Q., Yu, A., Lee, Y., and Zhang, J. (2019). Resource assignment based on dynamic fuzzy clustering in elastic optical networks with multi-core fibers. IEEE Transactions on Communications, 67(5), 3457-3469. https://doi.org/10.1109/TCOMM.2019.2894711
[64] Gao, J., Yi, X., Zhong, C., Chen, X., and Zhang, Z. (2019). Deep learning for spectrum sensing. IEEE Wireless Communications Letters, 8(6), 1727-1730. DOI: 10.1109/lwc.2019.2939314
[65] Liu, J., Wu, Q., Sui, X., Chen, Q., Gu, G., Wang, L., and Li, S. (2021). Research progress in optical neural networks: theory, applications and developments. PhotoniX, 2(1), 1-39. DOI:10.1186/s43074-021-00026-0
[66] Puttige, V. R., and Anavatti, S. G. (2007, August). Comparison of real-time online and offline neural network models for a uav. In 2007 International Joint Conference on Neural Networks (pp. 412-417). IEEE. DOI:10.1109/IJCNN.2007.4370992
[67] Althaf, C. M., and Prema, S. C. (2018, January). Covariance and eigenvalue based spectrum sensing using usrp in real environment. In 2018 10th International Conference on Communication Systems and Networks (COMSNETS) (pp. 414-417). IEEE. DOI:10.1109/COMSNETS.2018.8328231
[68] Thameur, H. B., and Dayoub, I. (2020). Real-Time In-Lab Test of Eigenvalue-Based Spectrum Sensing Using USRP RIO SDR Boards. IEEE Communications Letters, 25(3), 1029-1032. DOI: 10.1109/LCOMM.2020.3037010
[69] Astaneh, A. A., and Gheisari, S. (2018). Review and comparison of routing metrics in cognitive radio networks. Emerging Science Journal, 2(4), 191-201. DOI:10.28991/esj-2018-01143
[70] Berdnikov, V., and Lokhin, V. (2019). Synthesis of guaranteed stability regions of a nonstationary nonlinear system with a fuzzy controller. Civil Engineering Journal, 5(1), 107-116. DOI:10.28991/cej-2019-03091229
[71] Hai, T. N., Van, Q. N., and Tuyet, M. N. T. (2021). Digital Transformation: Opportunities and Challenges for Leaders in the Emerging Countries in Response to Covid-19 Pandemic. Emerging Science Journal, 5, 21-36. DOI:10.28991/esj-2021-SPER-03
[72] Chen, S., Zhong, S., Yang, S., and Wang, X. (2016). A multiantenna RFID reader with blind adaptive beamforming. IEEE Internet of Things Journal, 3(6), 986-996. DOI:10.1109/JIOT.2016.2542242
[73] Izydorczyk, T., Tavares, F. M., Berardinelli, G., and Mogensen, P. (2019). A USRP-based multi-antenna testbed for reception of multi-site cellular signals. IEEE Access, 7, 162723-162734. DOI:10.1109/ACCESS.2019.2952094